creative commons
COMMONS DEED

저작자표시-변경금지 2.0 대한민국

이용자는 아래의 조건을 따르는 경우에 한하여 자유롭게

- 이 저작물을 복제, 배포, 전송, 전시, 공연 및 방송할 수 있습니다.
- 이 저작물을 영리 목적으로 이용할 수 있습니다.

다음과 같은 조건을 따라야 합니다:

저작자표시. 귀하는 원저작자를 표시하여야 합니다.

변경금지. 귀하는 이 저작물을 개작, 변형 또는 가공할 수 없습니다.

- 귀하는, 이 저작물의 재이용이나 배포의 경우, 이 저작물에 적용된 이용허락조건을 명확하게 나타내어야 합니다.
- 저작권자로부터 별도의 허가를 받으면 이러한 조건들은 적용되지 않습니다.

저작권법에 따른 이용자의 권리는 위의 내용에 의하여 영향을 받지 않습니다.

이것은 이용허락규약(Legal Code)을 이해하기 쉽게 요약한 것입니다.

Disclaimer

dCollection

creative commons
COMMONS DEED

저작자표시-변경금지 2.0 대한민국

이용자는 아래의 조건을 따르는 경우에 한하여 자유롭게

- 이 저작물을 복제, 배포, 전송, 전시, 공연 및 방송할 수 있습니다.
- 이 저작물을 영리 목적으로 이용할 수 있습니다.

다음과 같은 조건을 따라야 합니다:

저작자표시. 귀하는 원저작자를 표시하여야 합니다.

변경금지. 귀하는 이 저작물을 개작, 변형 또는 가공할 수 없습니다.

- 귀하는, 이 저작물의 재이용이나 배포의 경우, 이 저작물에 적용된 이용허락조건을 명확하게 나타내어야 합니다.
- 저작권자로부터 별도의 허가를 받으면 이러한 조건들은 적용되지 않습니다.

저작권법에 따른 이용자의 권리는 위의 내용에 의하여 영향을 받지 않습니다.

이것은 이용허락규약(Legal Code)을 이해하기 쉽게 요약한 것입니다.

Disclaimer

dCollection

공학석사 학위논문

Out-of-plane Tension Behavior of CFT Column's Steel Tubular Wall for Component method

Component method 적용을 위한 CFT 기둥 강재판의 인장 거동 특성

2013년 7월

서울대학교 대학원

건축학과

김 상 우

Out-of-plane Tension Behavior of CFT Column's Steel Tubular Wall for Component method

지도 교수 홍 성 걸

이 논문을 공학석사 학위논문으로 제출함

20013 년 7 월

서울대학교 대학원

건축학과

김 상 우

김상우의 석사 학위논문을 인준함

2013 년 7 월

위 원 장 _____ (인)

부위원장 _____ (인)

위 원 _____ (인)

Abstract

Out-of-plane Tension Behavior of CFT Column's Steel Tubular Wall for Component method

Kim, Sangwoo
Department of Architecture
The Graduate School
Seoul National University

This paper is aiming to obtain the tension stiffness of the CFT column's plate to apply the component method to the semi-rigid connection including CFT column for more efficient design and precise analysis.

To obtain the tension stiffness of the CFT column's plate having infinite longitudinal length compared to transverse length, altered plate had been assumed. This plate has the finite length a with rigid connection for longitudinal direction, and column width length with simple boundary condition for transverse length. To find the assumed value a, making assumed plate's behavior similar to origin plate, a theoretical equation using plate theory had been derived and it had been compared to the numerical analysis. As a result, the assumed length a can be represented as proportion value to

column width, and the modification factor for bolt configuration has been obtained.

In addition to this basic model, adjusted theoretical equation and numerical analysis model considering end-plate effect had been developed with same procedure. To verify this effect, this numerical analysis model would have been verified by the comparison with experimental data.

As a result, the equation for tension stiffness of the CFT column's plate had been obtained, and this equation had been testified by comparison with the experimental data and numerical analysis. The assumed length a was determined as 0.7 times the width of the steel tube and these results can be applied to all dimensions of CFT column. In additions, the modification factor for loaded area had been earned through numerical analysis and it had been applied to the proposed equation.

And the proposed equation was applied to the semi-rigid beam-CFT column connection with bolt to show the example of design method using component method for semi-rigid joint.

Keywords: Component method, CFT column, Plate theory, tension stiffness, Experiment, Numerical Analysis, Semi-rigid connection
Student Number: 2011-23296

Contents

Chapter 1 Introduction 1

1.1 Research background 1

1.2 Research object 2

2.2 Research method 2

Chapter 2 Backgorund 4

2.1 Component method 4

2.1.1 Semi-rigid joints 4

2.1.2 Component method 5

2.1.3 Resistance of joints 9

2.1.4 Stiffness of joints 9

2.2 Plate theory 12

2.1.1 Equilibrium of plate element 12

2.1.2 Relationship between stress, strain and displacements 13

2.1.3 Governing equation for the plate 15

2.3 Former study 17

2.4 Bolt used in the connection of CFT column 18

Chapter 3 Suggestion of Theoretical Equation for the Deflection of CFT Column Plate with Tension Loading 21

3.1 Simplification of the CFT Column 21

3.1.1 Simplified model for CFT column 21

3.1.2 Assumed model for the plate theory 24

3.2 Theoretical equation for the CFT column under tension force with plate theory 25
3.2.1 Applying Navier's approach 25
3.2.2 Theoretical equation 28
3.2.3 Re-arrangement of the proposed equation 34

Chapter 4 Numerical Analysis for the Tension Strength of CFT Column 37
4.1 Complition of the theoretical equation 38
4.1.1 Finite element strategy 38
4.1.2 Abaqus set-up 39
4.1.3 Dimension of Abaqus models 39
4.1.4 Determining coefficient a 41
4.2 Modification factor for assumed loaded area 44
4.3 End-plate effect 48
4.3.1 Theoretical equation considering end-plate effect 48
4.3.2 Numerical analysis model for end plate effect 51
4.3.3 Test set-up and parameters 52
4.3.3 Result comparison 56
4.4 The equation for tension stiffness of the CFT column 58

Chapter 5 The Application of the Proposed Equation to the Component Method 63
5.1 The example of semi-rigid connection 63
5.2 The component identification 64
5.3 The component characteristics 65

5.3.1 The strength of the CFT column's plate 66
5.3.2 The characteristics of the CFT column in shear 72
5.4 The component assembly 76
Chapter 6 Conclusions 81

References 83

국문 초록 85

List of Tables

Table 4.1.1 Dimension of Numerical Analysis Model 40
Table 4.1.2 Deformation Results Comparison between proposed equation and numerical analysis..... 44
Table 4.2.1 Numerical analsis results: asumed area versus actual area..... 46
Table 4.3.1 Dimension of Experiment Model 53
Table 4.3.2 Strength and joint type of Experiment Model 54
Table 4.3.3 Numerical analysis results comparing to theoretical equaton..... 58
Table 4.4.1 The coefficient of the tension stiffness of CFT column plate for each loading case having same proportion ratio to column width b 59
Table 5.4.1 Design strength and Stiffness coefficients for components 77

List of Figures

Figure 1.1.1 Cross sectional diagram of CFT column 1
Figure 2.1.1 M-□ curve of joints: (a)Rigid joint (b)Simple joint (c)Semi-rigid joint 4
Figure 2.1.2 Boundaries for stiffness classification of beam-to-column joints. 5
Figure 2.1.3 Components represented by springs on bolted beam to column joint 6
Figure 2.1.4 F-δ curve of components 7
Figure 2.1.5 Assembling of components 8
Figure 2.1.6 Estimation of lever arm z for basic types of joints 9
Figure 2.1.7 Components of bolted beam-to-column joint, effective stiffness coefficients of bolt rows k_{eff} and equivalent stiffness of tension zone k_{eq} 11
Figure 2.2.1 External and internal forces on the element of middle surface ... 12
Figure 2.2.2 Stress on a plate element 14
Figure 2.3.1 Column web loaded area and equivalent strip of width l_{eff} 17
Figure 2.4.1 Detail of five-part Hollo-bolt mechanism (British Steel, 1997) . 19
Figure 2.4.2 Tightening of Hollow-bolt in a plain drilled hole 20
Figure 2.4.3 Stages of the Flowdrill process (British Steel, 1997) 20
Figure 3.1.1 Transform of CFT column to simplified model 22
Figure 3.1.2 Assumed loaded area 23
Figure 3.1.3 Cross sectional deformation after bolt tension test 23
Figure 3.1.4 Main deformation patterns of tubular section under tension 23
Figure 3.1.5 Assumed model to apply plate theory 25
Figure 3.2.2 Load condition for double trigonometric Series expansion 26
Figure 3.2.3 Central uniform load over rectangular plate 28
Figure 4.1.1 Finite element modeling 38

Figure 4.1.2 Numerical Analysis Model 40
Figure 4.1.3 Result(displacement) comparison between proposed equation and numerical analysis for case #1 41
Figure 4.1.4 Result(displacement) comparison between proposed equation and numerical analysis for case #2 42
Figure 4.1.5 Result(displacement) comparison between proposed equation and numerical analysis for case #3 42
Figure 4.1.6 Result(displacement) comparison between proposed equation and numerical analysis for case #4 43
Figure 4.1.7 Result(displacement) comparison between proposed equation and numerical analysis for case #5 43
Figure 4.2.1 Loaded area: (a) assumed area (b) bolt area 45
Figure 4.2.2 Loaded area in Aqaqus: (a) assumed area (b) bolt area 45
Figure 4.2.3 Abaqus data comparison: (a) assumed area (b) bolt area 47
Figure 4.2.4 Abaqus data comparison: (a) assumed area (b) bolt area 47
Figure 4.3.1 The boundary of the loaded area and measuring point g 48
Figure 4.3.2 Finite element modeling 52
Figure 4.3.3 Test layout (Neves 1996; Silva et al.2003) 54
Figure 4.3.4 Relevant geometrical characteristics of the joint 55
Figure 4.3.5 Result(displacement) comparison between proposed equation and numerical analysis for case E13 56
Figure 4.3.6 Result(displacement) comparison between proposed equation and numerical analysis for case E16 56
Figure 4.3.7 Result(displacement) comparison between proposed equation and numerical analysis for case E19 57
Figure 4.3.8 Result(displacement) comparison between proposed equation and numerical analysis for case E21 57
Figure 4.4.1 Result(displacement) comparison with proposed equation, experimental data, numerical analysis for case E13 60

Figure 4.4.2 Result(displacement) comparison with proposed equation, experimental data, numerical analysis for case E16 61
Figure 4.4.3 Result(displacement) comparison with proposed equation, experimental data, numerical analysis for case E19 61
Figure 4.4.3 Result(displacement) comparison with proposed equation, experimental data, numerical analysis for case E21 62
Figure 5.1.1 Semi-rigid connection with CFT column on transverse view 63
Figure 5.1.2 Semi-rigid connection with CFT column on longitudinal view . 64
Figure 5.2.1 Equivalent elastic system for the example..... 65
Figure 5.3.1 Yield line for CFT column's plate under bolt loading 67
Figure 5.3.2 Result(displacement) comparison between proposed equation and experimental data for case E13 71
Figure 5.3.3 Result(displacement) comparison between proposed equation and experimental data for case E16 71
Figure 5.3.4 Result(displacement) comparison between proposed equation and experimental data for case E19 72
Figure 5.3.5 STM model for CFT column in shear..... 73
Figure 5.3.6 STM model dimension for steel section of CFT..... 73
Figure 5.3.7 Load path for the transverse tension force by bolts 74
Figure 5.3.8 STM model dimension for concrete section of CFT 74
Figure 5.3.9 The geometry of STM model for CFT column in shear 76

Notations

a	Longitudinal assumed length of assumed model for CFT column
b	Width of CFT column
c	bolt diameter
d	Sum of the bolt diameter and the distance between bolts
D	$Eh^3/(1-\nu^2)$
E	Young's modulus
$F_{c.Rd}$	Design resistance in compression
$F_{t.Rd}$	Design resistance in tension
F_i	Force for components
F_{rd}	Design resistance
h	Thickness of the steel tube
k	Stiffness
k_i	stiffness coefficient for components
$k_{p,CFT,e}$	Tension stiffness of CFT column's plate with end-plate effect
M_m	Moment corresponding to the fixed end condtion
$M_{j,Rd}$	Design moment resistance
p	Lateral load on the plate
P	Total applied load to plate
P_{mn}	Lateral load coefficient
p_z	Distributed load
S_j	Rotational stiffness
$S_{j,ini}$	Initial rotational stiffness
w	Deflection of the plate
w_1	Deflection of the plate with simple boundary condition for all edges
w_2	Deflection of the plate due to transverse fixed end condition
$w_{p.max}$	Defection of the plate at center

$w_{p.CFT}$	Defection of the CFT's plate with end-plate effect
W_{mn}	Deflection coefficient
z	Lever arm
z_{eq}	Equivalent lever arm
α	Coefficient for a proportional to b
γ	Coefficient for c proportional to b
δ_{cd}	Deformation capacity
δ	Deformation of plate
δ_i	Deformation for components
ξ	Distance from the longitudinal boundary to the center of loaded area
η	Distance from the transverse boundary to the center of loaded area
κ	Tension stiffness coefficient
κ_1	Coefficient for the deflection w_1
κ_2	Coefficient for the deflection w_2
Ψ	Modification factor for assumed area
$\square_{Cd}$	Design rotation capacity
ν	Poisson ratio
χ	Coefficient for d proportional to b

Chapter 1. Introduction

1.1 Research background

Recently, the use of CFT column system, Concrete Filled Steel tube illustrated in Fig.1.1.1, in building structures has been increased due to its structural advantages. CFT column has outstanding resistance for compression, great resistance for torsion and local bucking because steel tube restrains the inside concrete and deduce the tri-axial stress. And it has little bearing force degradation and enhanced fire-proof ability.

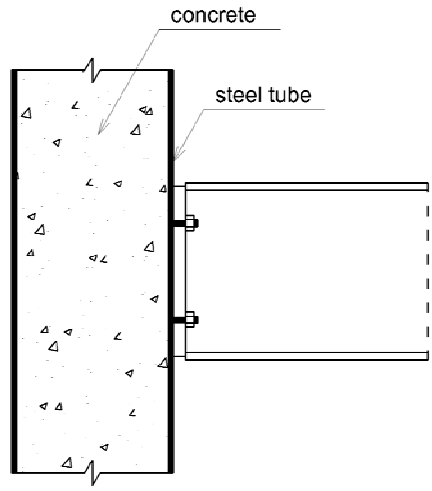

Fig. 1.1.1 Cross sectional diagram of CFT column

However, the design or analysis method for beam-CFT column joint is not well constructed practically. In most case, this beam-column joints has been considered rigid joints regardless of its connection type. The analytical and design method based on this

knowledge is not economical because it requires more stiffness and strength than actual case. To narrow this gap, the component method had been developed and applied to Eurocode from 1990's. The component method analyze the beam-column joint as semi-rigid connection with following procedure: divide the structure into each single component, apprehend the its characteristics and re-assemble these elements to find out the global structural behavior. Therefore, the design method for CFT column joint using component method is expected to have more efficiency and economic feasibility than existing method.

1.2 Research object

To apply the component method to the beam-column joint using CFT column, the characteristics of each components need to be defined. In case of the components in beam section, Eurocode had already suggested the proper design resistance and stiffness for these. In case of CFT Column, it can be divided into 5 components: steel tubular plate in tension(tension), concrete in tension, column in compression, concrete in shear and steel tube in shear. Among these components, this paper focuses on the characteristics of the steel tubular plate in tension(tension) because the other components had been already studied or cannot be standardized but obtained by experiments.

1.3 Research method

To obtain the tension stiffness of the CFT column's plate having infinite longitudinal

length compared to transverse length, altered plate had been assumed. This plate has the finite length a with rigid connection for longitudinal direction, and column width length with simple boundary condition for transverse length. To find the assumed value a, making assumed plate's behavior similar to origin plate, a theoretical equation using plate theory had been derived and it had been compared to the numerical analysis. As a result, the assumed length a can be represented as proportion value to column width, and the modification factor for bolt configuration has been obtained.

In addition to this basic model, adjusted theoretical equation and numerical analysis model considering end-plate effect had been developed with same procedure. To verify this effect, this numerical analysis model would have been verified by the comparison with experimental data. Through above process, the equation for the tension stiffness of CFT column's plate had been suggested and applied to composite semi-rigid joint with the other characteristics such as the tension strength of CFT plate and the shear strength and stiffness of CFT column.

Chapter 2. Background

2.1 Component method

2.1.1 Semi-rigid joints

Semi-rigid joints is the intermediate form between rigid joints not allowing the rotation of joint and simple(pinned) joints having no resistance to rotation. Conventionally, simplifying the connection as rigid or simple is quite popular because they have the advantage of straight-forward calculation. However, as modern design approaches evolve, those conventional calculation methods can be replaced by more advanced ones named semi-rigid joint. According to this new approach, joints may be assessed with regard to the following three main characteristics such as initial rotational stiffness ($S_{j,ini}$), design moment resistance ($M_{j,Rd}$) and design rotation capacity (ϕ_{Cd}), and each joint is compared in Fig.2.1.1 with these characteristics.

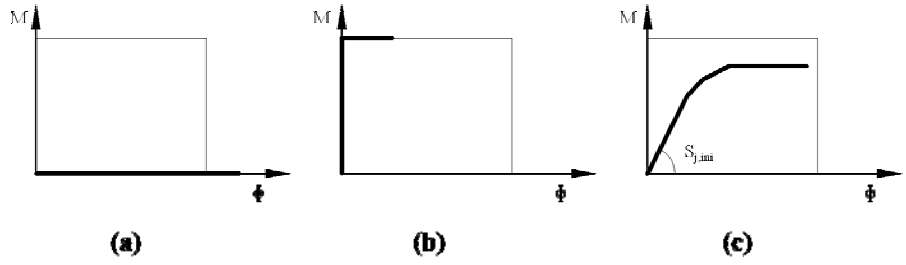

Fig. 2.1.1 M-ϕ curve of joints: (a)Rigid joint (b)Simple joint (c)Semi-rigid joint

For composite joints, the idealized classification would be ambiguous because the

relationships between its component cannot be perfectly defined as rigid or hinge. In this case, a beam-to-column joint can be classified as rigid, simple(pinned) or semi rigid according to its stiffness, $S_{j,ini}$. as indicated in Fig.2.1.2. If its stiffness ($S_{j,ini}$) is bigger than $8EI_b/L_b$, this connection would be classified as rigid connection(zone 1 in Fig.2.1.2) where EI_b is the uncracked flexural stiffness for a cross-section of a composite beam and L_b is the span of a beam (centre-to-centre of columns). .If its stiffness ($S_{j,ini}$) is less than $0.5EI_b/L_b$, this connection would be classified as hinge(pinned) connection, (zone 3 in Fig.2.1.2). And all joints in zone 2 in Fig.2.1.2 should be defined as semi-rigid joints in case of the composite joints.

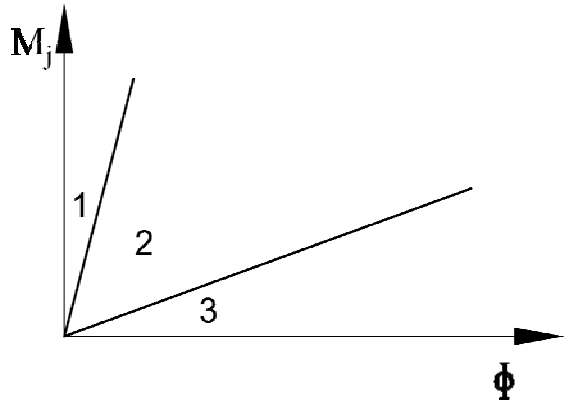

Fig. 2.1.2 Boundaries for stiffness classification of beam-to-column joints

2.1.2 Component method

The application of the component method requires three basic steps: listing of the joint components, evaluation of force-deflection diagram of each individual component, in terms of initial stiffness, strength and deformation capacity, and assembly of the

components in view to evaluate the whole joint behavior. The accuracy of the method depends on accuracy of the description of the basic components by independent springs and on the quality of the assembling.

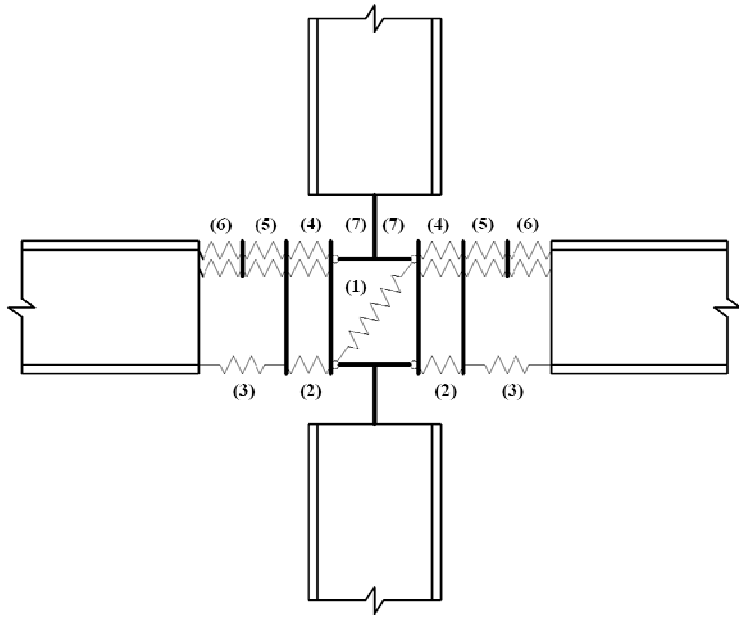

Fig. 2.1.3 Components represented by springs on bolted beam to column joint

To apply the component method to semi-rigid joint, the first step is to regard the joint as an assembly of a separate element of finite size, which called component identification. In this stage, each contributing components composing connection in compression, tension and shear in view of connecting elements and load are divided to each section. After subdividing, all the components in each section are separated to each component such as bolt, beam's web and column's flange. Fig.2.1.3 shows the example of these steps for bolted beam to column connection with following components: (1) unstiffened column web in shear, (2) unstiffened column web in compression, (3) beam

flange in compression, (4) column flange in bending, (5) bolt row in tension, (6) beam flange in bending and (7) unstffened column web in tension.

Next, subdivided component's individual force-deformation response need to be determined with the help of analytical mechanical models, components test or FEM-simulations, which calls component characterization. Behavior of the components can be described by non-linear force-deformation curve as indicated in Fig.2.1.1.(c). The behavior is often non-linear and includes various effects such as membrane effect and strain hardening, however, it can be simplified to bi-linear or tri-linear model as indicated in Fig.2.1.4. In this model, most important parameters are design resistance(F_{rd}), stiffness(k) and deformation capacity(δ_{cd}).

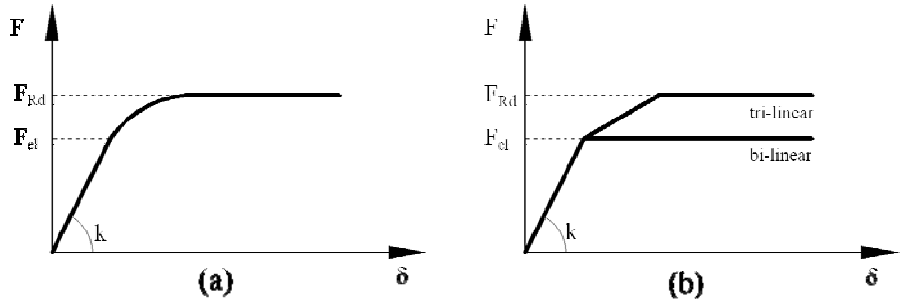

Fig. 2.1.4 F-δ curve of components: (a)non-linear models (b)linear models

Finally, these divided and characterized components need to be assembled to obtain properties of the semi-rigid joints. In practical application, the designer usually needs only initial stiffness and bending moment resistance of joints, and these can be gained through the assembling those components. In most case, the way of assembling these joints are defined as following two: parallel and serial configuration. When the

components are arranged in parallel configuration as Fig.2.1.5.(a), the resulting properties of the assembly can be gained as following.

$$\begin{aligned} F_{Rd} &= F_{1.Rd} + F_{2.Rd} \\ k &= k_1 + k_2 \\ \delta_{Cd} &= min(\delta_1 ; \delta_2) \end{aligned} \tag{2.1.1}$$

For components in serial configuration as Fig.2.1.5.(b), the following formulas can be applied.

$$\begin{aligned} F_{Rd} &= min(F_{3.Rd} ; F_{4.Rd}) \\ k &= \frac{k_3 \cdot k_4}{k_3 + k_4} \\ \delta_{Cd} &= \delta_3 + \delta_4 \end{aligned} \tag{2.1.2}$$

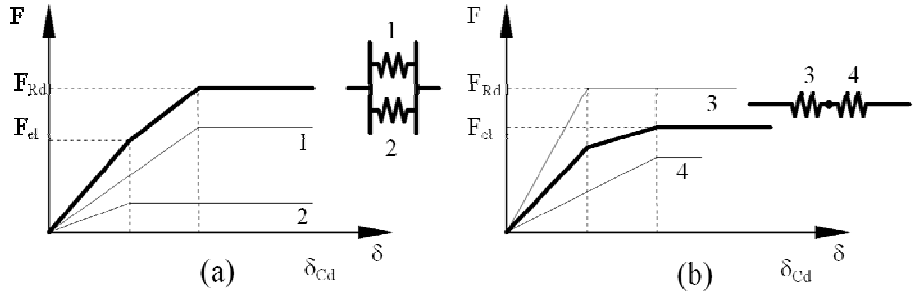

Fig. 2.1.5 Assembling of components: (a)Parallel configuration (b)Serial configuration

2.1.3 Resistance of joints

Bending moment resistance of joints is determined by the weakest component in tension, compression and shear zone. After applying component method mentioned in Chapter 2.1.2, the stiffness and the design resistance force for each section can be obtained. For each section, the minimum resistance force is the critical value. Comparing with these values, the moment resistance of each joints can be gained through the product of the minimum value of design resistance in tension, $F_{t.Rd}$ and design resistance in compression $F_{c.Rd}$ and the lever arm z as indicated in eq. 2.1.3. The lever arm, z, is different for each case and the example of this is illustrated at Fig.2.1.6.

$$M_{j.Rd} = min(F_{t.Rd}; F_{c.Rd}) \cdot z \tag{2.1.3}$$

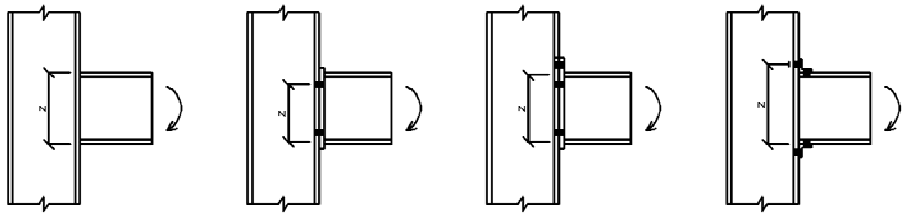

Fig. 2.1.6 Estimation of lever arm z for basic types of joints

2.1.4 Stiffness of joints

The component method can be used for calculation of initial stiffness of the joint, $S_{j.ini}$. The stiffness is calculated by adding elastic deformations of single components.

The deformation δ using stiffness coefficient k_i of the component is equal to

$$\delta_i = \frac{F_i}{k_i E} \tag{2.1.4}$$

Rotation of the joint can be calculated from deformation o9f the components taking into account lever arm between tension and compression zone as illustrated as Fig.2.1.8.

$$\phi_j = \frac{\sum_i \delta_i}{z} \tag{2.1.5}$$

Using previous formula, the stiffness of the joint can be obtained

$$S_j = \frac{M_j}{\phi_j} = \frac{F_i \cdot z}{\frac{\sum \delta_i}{z}} = \frac{F_i \cdot z^2}{\frac{F_i}{E}\sum \frac{1}{k_i}} = \frac{E \cdot z^2}{\sum \frac{1}{k_i}} \tag{2.1.6}$$

The effective stiffness coefficient k_{eff} of every bolt row in tension should be calculated from

$$k_{eff} = \frac{1}{\sum \frac{1}{k_i}} \tag{2.1.7}$$

where k_i are stiffness coefficient of basic components considered for the particular

bolt row. Usually, these are unstiffened column web in tension, column flange in bending, bolts in tension and end plate in bending.

Fore end plate connections with two or more bolt rows in tension, the basic components of all bolt rows are represented by a single equivalent stiffness k_{eq} determined from

$$k_{eq} = \frac{\sum_j k_{eff.j} z_i}{z_{eq}} \tag{2.1.8}$$

The equivalent lever arm z_{eq} should be determined from

$$z_{eq} = \frac{\sum_j k_{eff.j} z_j^2}{\sum_j k_{eff.j} z_j} \tag{2.1.9}$$

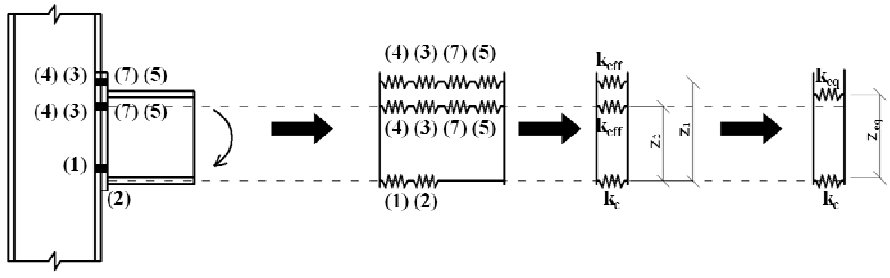

Fig. 2.1.7 Components of bolted beam-to-column joint, effective stiffness coefficients of bolt rows k_{eff} and equivalent stiffness of tension zone k_{eq}

2.2 Plate theory

2.2.1 Equilibrium of plate element

To derive the governing equation of thin plates, an elemental beam theory would be used because the behavior of the plate is similar to that of a two-dimensional grid work of beams as shown at Fig.2.2.1.

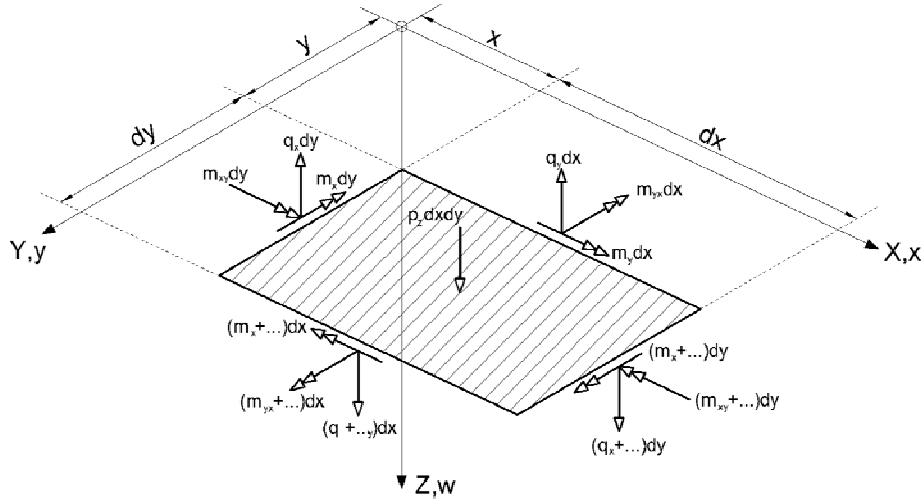

Fig. 2.2.1 External and internal forces on the element of the middle surface

In Fig.2.2.1, the sum of the moments of all forces around the X, Y and Z axis is zero. This condition gives following Eq.2.2.1 about X, Y and Z axis after simplification, respectively.

$$\frac{\partial m_x}{\partial x}+\frac{\partial m_{yx}}{\partial y}=q_x,\ \ \frac{\partial m_y}{\partial x}+\frac{\partial m_{xy}}{\partial y}=q_y,\ \ \frac{\partial q_x}{\partial x}+\frac{\partial q_y}{\partial y}=-p_z \tag{2.2.1}$$

Substituting the equation about X and Y axis of Eq.2.2.1 to the equation about z axis of Eq.2.2.1 with $m_{xy}=m_{yx}$,

$$\frac{\partial^2 m_x}{\partial x^2}+2\frac{\partial^2 m_{xy}}{\partial x\partial y}+\frac{\partial^2 m_y}{\partial y^2}=-p_z(x,y) \tag{2.2.2}$$

The bending and twisting moments in Eq.2.2.2 depend on strains, and the strains are the function of the displacement components (u, v, w). Thus, in the next steps. relationships between the internal moments and displacement components are sought.

2.2.1 Relationship between stress, strain and displacements

The bending and twisting moments in Eq.2.2.2 depend on strains, and the strains are the function of the displacement components (u, v, w). Thus, in the next steps. relationships between the internal moments and displacement components are sought. The stress of X and Y axis and shear stress would be expressed as following from Eq.2.2.3 to Eq. 2.2.5 if elasticity of material is assumed.

$$\sigma_x=\frac{E}{1-\nu^2}\left(\varepsilon_x+\nu\varepsilon_y\right) \tag{2.2.3}$$

$$\sigma_y = \frac{E}{1-\nu^2}\left(\varepsilon_y + \nu\varepsilon_x\right) \tag{2.2.4}$$

$$\tau_{xy} = \frac{E}{2(1+\nu)}\gamma_{xy} \tag{2.2.5}$$

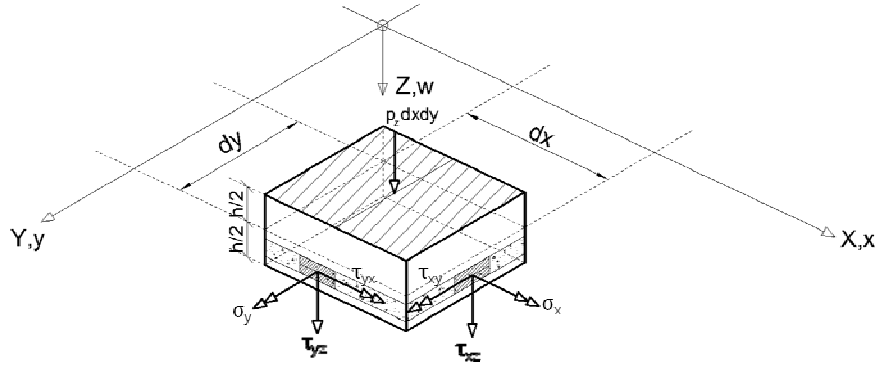

Fig. 2.2.2 Stress on a plate element

The strain of each axis can be defined as following from Eq. 2.2.6 to Eq. 2.2.8.

$$\varepsilon_x = -z\frac{\partial^2 w}{\partial x^2} \tag{2.2.6}$$

$$\varepsilon_y = -z\frac{\partial^2 w}{\partial y^2} \tag{2.2.7}$$

$$\gamma_{xy} = -2z\frac{\partial^2 w}{\partial x \partial y} \tag{2.2.8}$$

2.2.3 Governing equation for the plate

The stress components σ_x and σ_y produce bending moments in the plate element in a manner similar to that in elementary beam theory. Thus, by integration of normal stress components, the bending moments, acting on the plate element, are obtained.

$$m_x = \int_{-(h/2)}^{+(h/2)} \sigma_x z dz, \quad m_y = \int_{-(h/2)}^{+(h/2)} \sigma_y z dz \tag{2.2.9}$$

Similarly, the twisting moments produced by the shear stress $\tau = \tau_{xy} = \tau_{yx}$ can be calculated from

$$m_{xy} = m_{yx} = \int_{-(h/2)}^{+(h/2)} \tau_{xy} z dz \tag{2.2.10}$$

Substituting Eq. 2.2.6 and Eq. 2.2.7 into Eq. 2.2.3 and Eq.2.2.4, the normal stress σ_x and σ_y are expressed in terms of the lateral deflection w as Eq. 2.2.11 and Eq.2.2.12.

$$\sigma_x = -\frac{E}{1-\nu^2}\left(\frac{\partial^2 w}{\partial x^2} + \nu \frac{\partial^2 w}{\partial y^2}\right) \tag{2.2.11}$$

$$\sigma_y = -\frac{E}{1-\nu^2}\left(\frac{\partial^2 w}{\partial y^2} + \nu \frac{\partial^2 w}{\partial x^2}\right) \tag{2.2.12}$$

After substitution of Eq.2.2.11 and Eq.2.2.12 into Eq. 2.2.9, the integration of it would be result in as follow:

$$m_x = -\frac{Eh^3}{12\left(1-\nu^2\right)}\left(\frac{\partial^2 w}{\partial x^2}+\nu\frac{\partial^2 w}{\partial y^2}\right) = -D\cdot\left(\frac{\partial^2 w}{\partial x^2}+\nu\frac{\partial^2 w}{\partial y^2}\right) \tag{2.2.13}$$

$$m_y = -\frac{Eh^3}{12\left(1-\nu^2\right)}\left(\frac{\partial^2 w}{\partial y^2}+\nu\frac{\partial^2 w}{\partial x^2}\right) = -D\cdot\left(\frac{\partial^2 w}{\partial y^2}+\nu\frac{\partial^2 w}{\partial x^2}\right) \tag{2.2.14}$$

Here, the coefficient D, representing the flexural of the plate, is defined as

$$D = \frac{Eh^3}{12\left(1-\nu^2\right)} \tag{2.2.15}$$

In a similar manner, the expression of twisting moment in terms of the lateral deflections is obtained:

$$m_{xy} = m_{yx} = -\left(1-\nu\right)\frac{Eh^3}{12\left(1-\nu^2\right)}\frac{\partial^2 w}{\partial x\partial y} = -\left(1-\nu\right)\cdot D\cdot\frac{\partial^2 w}{\partial x\partial y} \tag{2.2.16}$$

Substituting Eq. 2.2.13, Eq. 2.2.14 and Eq. 2.2.16 into Eq. 2.2.2 yields the governing equation of the plate subjected to distributed lateral loads as Eq. 2.2.17

$$\frac{\partial^4 w}{\partial x^4} + 2\frac{\partial^4 m_{xy}}{\partial x^2 \partial y^2} + \frac{\partial^4 w}{\partial y^4} = \frac{p_z(x,y)}{D} \tag{2.2.2}$$

2.3 Former study

For the behavior of minor axis beam-to-column semi-rigid joints, Neves and Gomes (1996) concluded that the column web of minor axis joints could be modeled as a plate supported at the junction with the flanges and free in the other borders. And for the rotational stiffness of rectangular hollow sections composite joints, they had concluded that same model as the former can be used for the latter. They assumed the plate has a length L and a width l_{eff} as Eq.2.3.1 and Eq. 2.3.2. and this is illustrated at Fig.2.3.1.

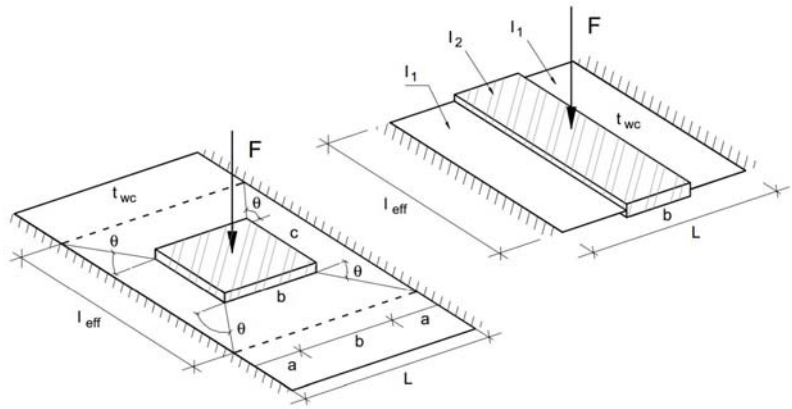

Fig. 2.3.1 Column web loaded area and equivalent strip of width l_{eff}(Neves and Gomes.1996)

$$l_{eff} = c + (L - b)\tan\theta$$
$$\frac{l_{eff}}{L} = \alpha + (1 - \beta)\tan\theta \tag{2.3.1}$$

$$a = \frac{1}{2}(L - b) \tag{2.3.1}$$

The theoretical initial stiffness of this strip, including both flexural and shear deformations, is defined as Eq. 2.3.3

$$S_i = \frac{2El_{eff}t_{wc}^3}{a^3 + 2(1+\nu)at_{wc}^2} \tag{2.3.3}$$

Substituting Eq.2.3.1 and Eq.2.3.2 into Eq. 2.3.3 with the poisson ratio ν=0.3, and introducing coefficients k_1 and k_2, the following equation can be earned

$$S_i = \frac{Et_{wc}^3}{L^2} 16 \frac{\alpha + (1-\beta)\tan\theta}{(1-\beta)^3 + 10.4(k_1 - k_2\beta)/(L^2/t_{wc}^2)} \tag{2.3.4}$$

Even though those coefficients k1 and k2 is agreed to 1.5 and1.63, respectively, and the relationship between θ and β is defined as θ=35-10β, this equation is hard to be applied to the CFT column practically. That's because this equation contains many coefficient and ambiguous definition of θ. Thus, The simple and definite equation for the stiffness of the CFT column's plate need to be derived for practical usages.

2.4 Bolt used in the connection of CFT Column

The tubular column and CFTcolumn's usages is limited due to their disadvantages in connection assembly even though they offer various structural advantages as mentioned in Chapter 1. The traditional bolts and nuts cannot be used for this connection on account of the restricted access of the internal face. To overcome this disadvantage, blind-bolting technologies such as Hollo-Bolt and Flowdrill had been developed (British Steel, 1997), and description of both technologies are given below.

Hollo-Bolt, shown at Fig.2.4.1, is a pre-assembled three or five-part fastner that is inserted into plain drill holes. The tightening of the bolt due to the fastner draws the cone into the body which spreads the legs to form a secure fixing as illustrated in Fig.2.4.2.

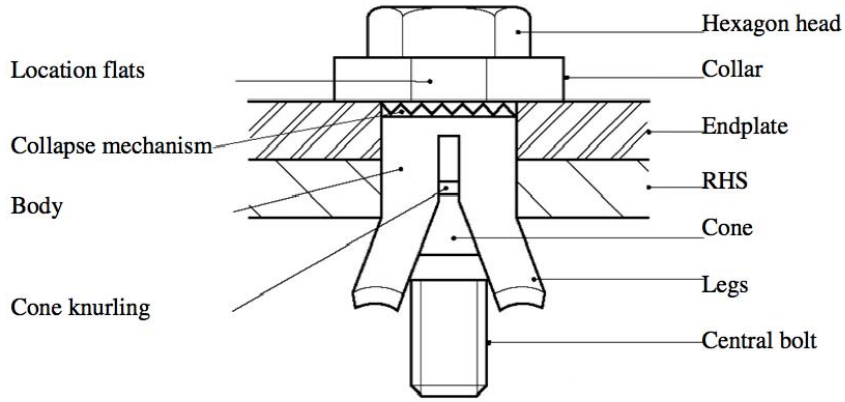

Fig. 2.4.1 Detail of five-part hollo-bolt mechanism (British Steel, 1997)

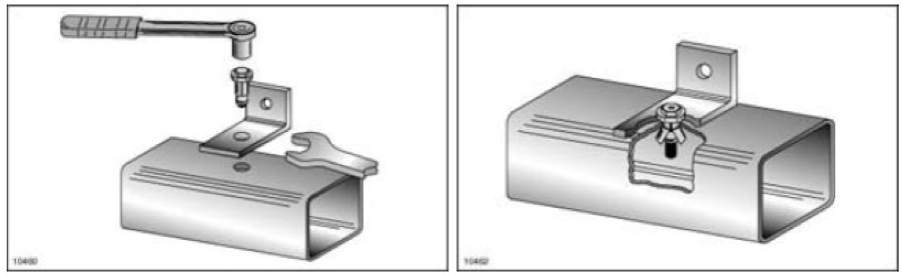

Fig. 2.4.2 Tightening of hollo-bolt in a plain drilled hole (British Steel, 1997)

Flowdrilling consists of a thermal drilling process and tapping of threads to accept a standard threaded bolt as shown in Figure 2.4.3. During the thermal drilling stage (1st stage), material is displaced forming a hole and internal brushing. While the second phase, the hole is tapped using a roll thread-forming tool called a "Coldfrom Flowtrap). This method can be used effectively with column faces with thickness as low as 6mm (British steel, 1997).

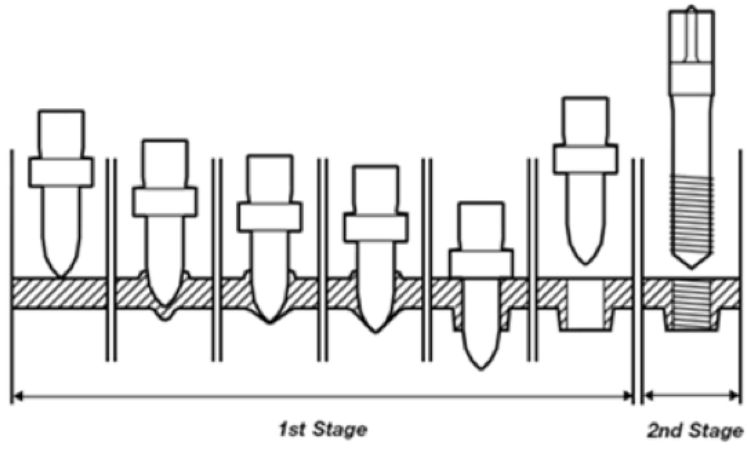

Fig. 2.4.3 Stages of the flowdrill process (British Steel, 1997)

Chapter 3. Suggestion of Theoretical Equation for the Deflection of CFT Column plate with Tension Loading

3.1 Simplification of the CFT column

3.1.1 Simplified model for the CFT column

The rectangular CFT column's tension stiffness can be analyzed by plate theory after transforming its shape to simplified one considering boundary condition. In view of the component method, this column is composed of two components: a steel tubular section and a rectangular parallelepiped concrete section. As illustrated in Fig.1.1.1, CFT column is including components as follow: bending of tubular section, concrete section in shear, concrete section in compression, steel tubular section in compression, concrete section in tension. Practically, except the component of tension of the plate, the other components have the infinite value of strength. Which means that tension strength of the steel tubular section is only one we need to concern to apply the component method to CFT semi-rigid joint. To gain the value of this, CFT column with bolt-connection joint can be idealized to Fig.3.1.1(a) only concerning the tension of the steel section's plate. The boundary condition of the loaded plate on transverse direction can be assumed as fixed because the concrete filled inside of steel tubular section hold the deformation of side plates to its direction different from tubular steel hollow section. In case of longitudinal direction, it can be assumed to have the infinite length on its direction because the length of it is far longer than bolt diameter or longitudinal distance

between bolts. Thus, Fig.3.1.1(a) can be simplified to Fig.3.1.1(b) to obtain the tension strength of the plate.

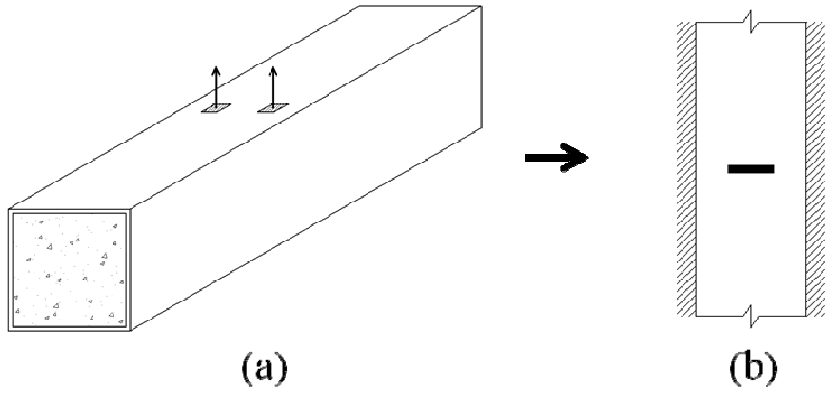

Fig. 3.1.1 Transform of CFT column to simplified model: (a)Actual CFT column, (b) Simplified rectangular CFT column plate

In Fig.3.1.1(a), solid hatched area and arrow indicates the loaded area by bolt and its direction, respectively. This distributed load area by bolt need to be transformed to extended area with equal magnitude as illustrated in Fig.3.1.1(b). This assumption, transforming separate loaded areas by bolt into rectangular area surrounded distance between bolts, can be justified because a deformed geometry of plate between bolts is retained as plain or angle by end plate as illustrated in Fig.3.1.3 and Fig.3.1.4, a deformed geometry of plate between bolts is retained as plain by end plate. Also, this assumption is very efficient to obtain the tension stiffness of the plate using the plate theory. And the relative error due to this assumption would be modified through modification factor in Chapter 4.3.2.

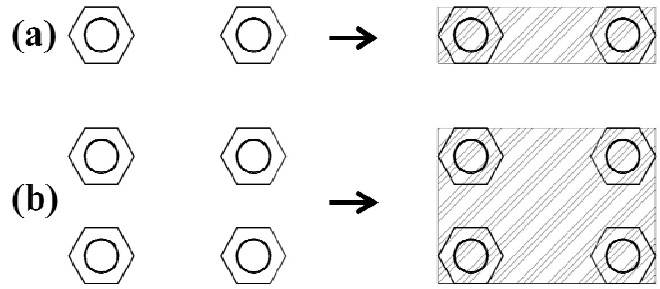

Fig. 3.1.2 Assumed loaded area

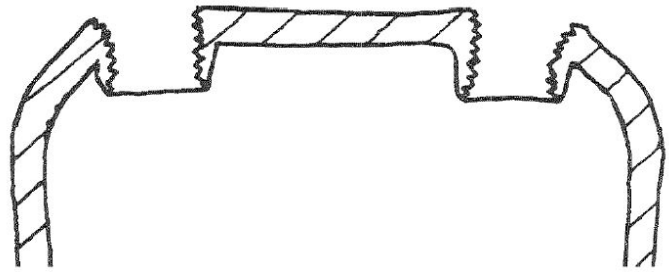

Fig. 3.1.3 Cross sectional deformation after bolt tension test (British steel)

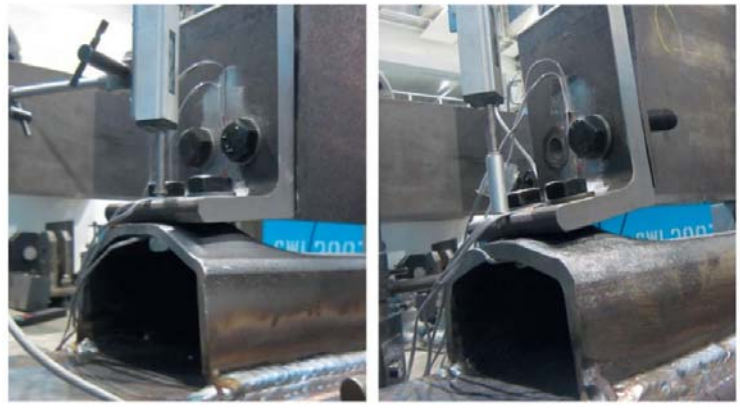

Fig. 3.1.4 Main deformation patterns of tubular section under tension (Y. Liu et al. 2012)

3.1.2 Assumed model for the plate theory

To obtain the tension stiffness of the plate of the CFT column, we can use the plate theory suggested by Navier. In 1820, he presented a paper on the solution of bending of simply supported rectangular plates by double trigonometric series. We should modify an actual model to an idealized shape to apply the Navier's approach due to his assumption. In Navier's approach of the plate theory, he analyzed the rectangular plate having simply supported edge conditions at all edges. The boundary condition of rectangular plates, for which the Navier solution is applicable, are representing simply supported edge conditions at all edges as indicated in Eq.3.1.1.

$$\begin{aligned} &(w)_{x=0.x=a} = 0, \ \ (m_x)_{x=0.x=a} = 0, \\ &(w)_{y=0.y=a} = 0, \ \ (m_y)_{y=0.y=a} = 0 \end{aligned} \tag{3.1.1}$$

To satisfy the assumption of Navier's approach for our simplified CFT model, it need to be converted to the plate having simple supported boundary condition for all edges. In case of longitudinal direction, infinite length of plate can be converted in to the member having simple supported boundary on both side with virtual finite length a as fig.3.1.5(a). Because this assumed plate's behavior need to be similar as origin, the assumed length a need to be determined by the comparison with numerical analysis and experiment data. In case of transverse boundary condition, we can modify fixed end boundary condition into superposition of simple support and moment action corresponding to fixed end boundary condition shown as Fig.3.1.5(c). By these assumption and assumed model as Fig.3.1.5, simplified rectangular CFT column can be

applied to plate theory to obtain the tension stiffness of CFT column.

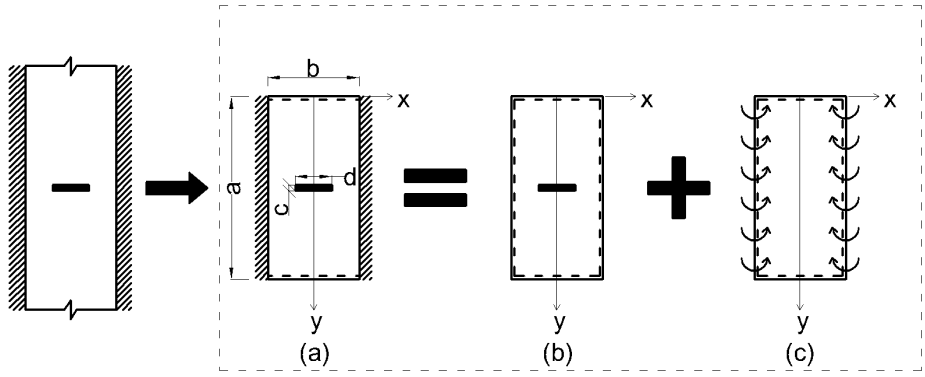

Fig. 3.1.5 Assumed model to apply plate theory

3.2 Theoretical equation for the CFT column under tension force with plate theory

3.2.1 Applying Navier's approach

The solution of the governing differential equation of the plate (Eq.2.2.2) subjected to a transverse loading is obtained by Navier's method as follows;

1. The deflections are expressed by a double sine series,

$$w(x,y)=\sum_{m=1}^{\infty}\sum_{n=1}^{\infty}W_{mn}\sin\frac{m\pi x}{a}\sin\frac{n\pi y}{b} \tag{3.2.1}$$

which satisfies all the boundary conditions (simple supported) indicated in Eq.3.1.1.

In Eq.3.2.1, the coefficient of the deflection W_{mn} is unknown yet.

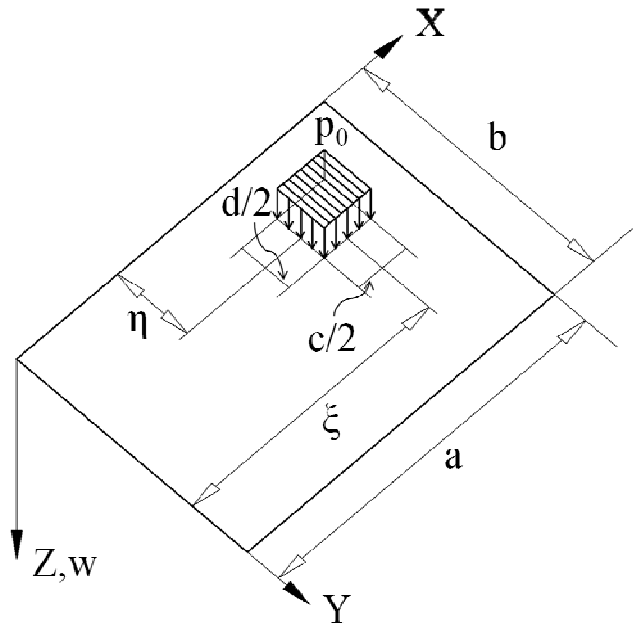

Fig. 3.2.2 Load condition for double trigonometric Series expansion

2. The lateral load p_z is also expanded into a double sine series:

$$p_z(x,y) = \sum_{m=1}^{\infty}\sum_{n=1}^{\infty} P_{mn} \sin\frac{m\pi x}{a}\sin\frac{n\pi y}{b} \tag{3.2.2}$$

The coefficients P_{mn} of the Fourier expansion of the load can be defined as Eq.3.2.3 and the case shown at Fig.3.2.1 because the tensile load resulting from bolt is assumed as rectangular equally distributed load as indicated in Fig.3.1.2.

$$P_{mn} = \frac{16 p_0}{\pi^2 mn} \sin\frac{m\pi\xi}{a} \sin\frac{n\pi\eta}{b} \sin\frac{m\pi c}{2a} \sin\frac{n\pi d}{2b} \qquad (3.2.3)$$
$$for \quad m,n = 1,2,3...$$

3. Substituting Eqs. (3.2.1) and (3.2.2) into the governing differential equation (2.2.2), an algebraic equation is obtained from which the unknown W_{mn} can be easily calculated.

$$W_{mn}\left[\frac{m^4\pi^4}{a^4} + \frac{m^2n^2\pi^4}{a^2b^2} + \frac{n^4\pi^4}{b^4}\right] \sin\frac{m\pi x}{a} \sin\frac{n\pi y}{b} = \frac{1}{D} P_{mn} \sin\frac{m\pi x}{a} \sin\frac{n\pi y}{b} \qquad (3.2.5)$$

hence

$$W_{mn} = \frac{P_{mn}}{D\pi^4\left[\left(m^2/a^2\right)+\left(n^2/b^2\right)\right]^2} \qquad (3.2.6)$$

Summing the individual terms, an analytical solution for the deflection of the plate is obtained. Thus we can write

$$w(x,y) = \frac{1}{D\pi^4} \sum_{m=1}^{\infty}\sum_{n=1}^{\infty} \frac{P_{mn}}{D\pi^4\left[\left(m^2/a^2\right)+\left(n^2/b^2\right)\right]^2} \cdot \sin\frac{m\pi x}{a} \sin\frac{n\pi x}{b} \qquad (3.2.7)$$

3.2.2 Theoretical equation

To obtain the tension strength of CFT column's plate, the deflection around loaded area is required. However, this paper suggests will obtain the deflection of the center of the loaded area. That's because not only the location of bolt can be altered for each case but also this detoured method can reduce the course of calculation with simple form. Later, the modification factor would be multiplied to this value to reflect this simplification. In this chapter, two sort of deflection, w_1 and w_2, would be obtained. The value of w_1 is the deflection when the plate is simple supported for all edges with assumed rectangular tension load as Fig.3.1.5(b). The value of w_2 is the deflection due to the moment corresponding to the applied load. The deflection of the center of loaded area would be obtained through the sum of these two values

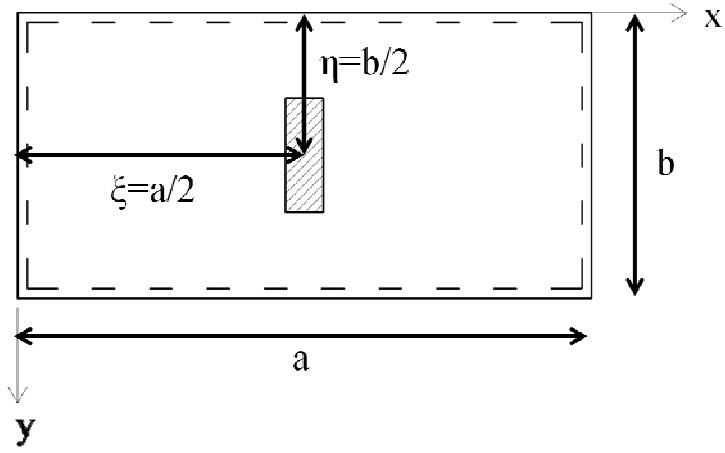

Fig. 3.2.3 Central uniform load over rectangular plate

For obtaining the deflection w_1, the coefficients P_{mn} of the Fourier expansion of the

lateral load need to be defined first for applying Navier's approach. Because the loaded area is assumed as rectangular shape and the located at the center of the plate as Fig.3.2.3, the value of ξ and η in Fig.3.2.2 should be a/2 and b/2, respectively. Then the coefficients P_{mn} can be earned though substituting these values into the Eq. 3.2.3.

$$P_{mn} = \frac{16 p_0}{\pi^2 mn} \sin\frac{m\pi}{2} \sin\frac{n\pi}{2} \sin\frac{m\pi c}{2a} \sin\frac{n\pi d}{2b} \qquad (3.2.8)$$
$$for \quad m,n = 1,2,3...$$

Substituting the value of P_{mn} obtained from Eq.3.2.8 into the Eq.3.2.6, then the coefficient of the deflection W_{mn} can be expressed as Eq.3.2.9.

$$W_{mn} = \frac{16 p_0 \sin\frac{m\pi}{2} \sin\frac{n\pi}{2} \sin\frac{m\pi c}{2a} \sin\frac{n\pi d}{2b}}{D\pi^6 mn\left[\left(m^2/a^2\right)+\left(n^2/b^2\right)\right]^2} \qquad (3.2.9)$$

Substituting W_{mn} into Eq.3.2.1, equation for the w_1, the deflection when all the boundaries are simple, can be obtained:

$$w_1(x,y) = \frac{16 p_0}{D\pi^6} \sum_{m=1}^{\infty}\sum_{n=1}^{\infty} \frac{\sin\left(\frac{m\pi}{2}\right)\sin\left(\frac{n\pi}{2}\right)\sin\left(\frac{m\pi c}{2a}\right)\sin\left(\frac{n\pi d}{2b}\right)}{mn\left[\left(m^2/a^2\right)+\left(n^2/b^2\right)\right]^2} \times \sin\frac{m\pi x}{a} \sin\frac{n\pi y}{b} \qquad (3.2.11)$$

To present the boundary condition of CFT column, as mentioned before, it could be modified as superposition of simple support and moment action corresponding to fixed end boundary condition shown as fig.3.1.5(c). This corresponding moment can be derived from the condition that the rotation induced by the external load have the same value but be opposite sign of the rotation induced by this moment both at its fixed boundary.

Consider a simply supported rectangular plate subjected to symmetrically distributed edge moment at y=+b/2, -b/2 as Fig.3.1.5(c), this moment can be described by Fourier sine series as follow:

$$f(x)=\sum_{m=1}^{\infty} M_m \sin\frac{m\pi x}{a} \tag{3.2.12}$$

Here M_m represent the unknown set of coefficients

$$M_m=\frac{2}{a}\int_0^a f(x)\sin\frac{m\pi x}{a}dx \tag{3.2.13}$$

The boundary conditions are

$$\begin{aligned} &w=0 \qquad \frac{\partial^2 w}{\partial x^2}=0 \qquad (x=0, x=a) \\ &w=0 \qquad -D\frac{\partial^2 w}{\partial x^2}=f(x) \qquad \left(y=\pm\frac{b}{2}\right) \end{aligned} \tag{3.2.14}$$

The solution next proceeds with an assumption of the deflection surface in the form

of simply supported rectangular plate under uniform loading with p_0=0, the deflection induced by the moment M_m (w_2) is induced as follow where α_m=mπb.

$$w_2 = \frac{a}{2\pi D}\sum_{m=1}^{\infty}\frac{sin(m\pi x/a)}{m\cdot cosh\,\alpha_m}M_m\left(\frac{b}{2}tanh\,\alpha_m\cdot cosh\frac{m\pi y}{a} - y\,sinh\frac{m\pi y}{a}\right) \tag{3.2.15}$$

We can induce M_m of w_2 with the condition that the rotation of bent plate alongside y=b/2 induced by p_0 and M_m must be zero because we establish the boundary condition of y=b/2 is fixed.

The x-y coordinate system of Eq.3.2.11 and Eq.3.2.15 is different. For comparing the rotations induced by these equation to obtain the corresponding moment, the coordinate system of Fig.3.2.3 need to be transformed to the that of Fig.3.1.5. If the origin of the coordinate system in Fig.3.2.3 is moved to x=0 and y=b/2, this coordinate system would be same as Fig.3.1.5(b). Then Eq.3.2.11, about the deformation of w_1, in new coordinate system can be described as follow:

$$w_1(x,y) = \frac{16p_0}{D\pi^6}\sum_{m=1}^{\infty}\sum_{n=1}^{\infty}\frac{sin\left(\frac{m\pi}{2}\right)sin\left(\frac{n\pi}{2}\right)sin\left(\frac{m\pi c}{2a}\right)sin\left(\frac{n\pi d}{2b}\right)}{mn\left[\left(m^2/a^2\right)+\left(n^2/b^2\right)\right]^2} \times sin\frac{m\pi x}{a}sin\frac{n\pi}{b}\left(y+\frac{b}{2}\right) \tag{3.2.16}$$

The rotation of the bent plate along the side y=b/2 induced by p_0 is

$$\frac{\partial w_1}{\partial y}\left(y=\frac{b}{2}\right)=\frac{16p_0}{D\pi^6}\sum_{m=1}^{\infty}\sum_{n=1}^{\infty}\frac{\sin\left(\frac{m\pi}{2}\right)\sin\left(\frac{n\pi}{2}\right)\sin\left(\frac{m\pi c}{2a}\right)\sin\left(\frac{n\pi d}{2b}\right)}{mn\left[\left(m^2/a^2\right)+\left(n^2/b^2\right)\right]^2}$$
$$\times\sin\frac{m\pi x}{a}\cdot\frac{n\pi}{b}\cdot(-1) \tag{3.2.17}$$

And the rotation of the bent plate along the side y=b/2 induced by M_m is

$$\frac{\partial w_2}{\partial y}\left(y=\frac{b}{2}\right)=\frac{a}{2\pi D}\sum_{m=1,3..}^{\infty}\frac{1}{m}M_m\left[\tanh\alpha_m\left(\alpha_m\tanh\alpha_m-1\right)-\alpha_m\right]\cdot\sin\frac{m\pi x}{a} \tag{3.2.18}$$

The requirements that the slopes for both plates at y=b/2 have the same value but be of opposite sign is satisfied if

$$\frac{\partial w_1}{\partial y}=-\frac{\partial w_2}{\partial y}\qquad\left(y=\pm\frac{b}{2}\right) \tag{3.2.19}$$

Now, we can get M_m through substituting Eq.3.2.17 and Eq.3.2.18 into Eq.3.2.19

$$M_m = \frac{32 p_0}{ab\pi^4} \cdot \frac{\sin(m\pi/2)\cdot\sin(c/a)\cdot(m\pi/2)}{\left[\tanh\alpha_m\left(\alpha_m \tanh\alpha_m - 1\right) - \alpha_m\right]} \times \sum_{n=1,3..}^{\infty} \frac{\sin\frac{n\pi}{2}\cdot\sin\left(\frac{d}{b}\cdot\frac{n\pi}{2}\right)}{\left[\left(m^2/a^2\right)+\left(n^2/b^2\right)\right]^2} \tag{3.2.20}$$

Deflection induced by $M_m(w_2)$, which is result from p_0 and fixed condition, can be obtained by substituting Eq.3.2.20 to Eq.3.2.15

$$w_2 = \frac{8 p_0}{\pi^5 D} \sum_{m=1,3..}^{\infty} \sum_{n=1,3..}^{\infty} \frac{\left(\tanh(\alpha_m)\cdot\cosh\left(\frac{m\pi y}{a}\right) - y\sinh\frac{m\pi y}{a}\right)\cdot\sin\left(\frac{m\pi x}{a}\right)}{m\cdot\cosh\alpha_m\cdot\left[\tanh\alpha_m\left(\alpha_m\tanh\alpha_m - 1\right) - \alpha_m\right]} \times \frac{\sin\left(\frac{m\pi}{2}\right)\cdot\sin\left(\frac{c}{a}\cdot\frac{m\pi}{2}\right)\cdot\sin\left(\frac{n\pi}{2}\right)\cdot\sin\left(\frac{d}{b}\cdot\frac{n\pi}{2}\right)}{\left[\left(m^2/a^2\right)+\left(m^2/a^2\right)\right]^2} \tag{3.2.21}$$

The deflection of the plate, w_p, can be earned by summing of these two equations with substituting proper x and y value to Eq.(11) and Eq. (19) as follow:

$$w_p = w_1 + w_2 \tag{3.2.22}$$

The maximum deflection would be occurred at the center of the plate, and it can be eared The tension stiffness of this plate can be earned by this deflection, w_p, with

substituting the central coordinate, x=a/2 and y=0, then Eqs.3.2.20, 3.2.21 and 3.2.22 can be written as:

$$w_1\left(\frac{a}{2},0\right)=\frac{16p_0}{D\pi^6}\sum_{m=1,3..}^{\infty}\sum_{n=1,3..}^{\infty}\frac{sin(m\pi c/2a)\cdot sin(n\pi d/2b)}{mn\left[\left(m^2/a^2\right)+\left(n^2/b^2\right)\right]^2} \tag{3.2.23}$$

$$w_2\left(\frac{a}{2},0\right)=\frac{8p_0}{\pi^5 D}\sum_{m=1,3..}^{\infty}\sum_{n=1,3..}^{\infty}\frac{tanh(\alpha_m)\cdot sin\left(\frac{c}{a}\cdot\frac{m\pi}{2}\right)\cdot sin\left(\frac{n\pi}{2}\right)\cdot sin\left(\frac{d}{b}\cdot\frac{n\pi}{2}\right)}{m\cdot cosh\,\alpha_m\cdot\left[tanh\,\alpha_m\left(\alpha_m\,tanh\,\alpha_m-1\right)-\alpha_m\right]} \times\frac{1}{\left[\left(m^2/a^2\right)+\left(m^2/a^2\right)\right]^2} \tag{3.2.24}$$

$$w_{p,max}=w_1+w_2 \tag{3.2.25}$$

3.2.3 Re-arrangement of the proposed equation

The coefficients a, c and d in Eq.3.2.23, and Eq.3.2.24, which are the dimension of load area and plate, are related to each other and column width b. In case of a, this value is proportional to b as to assume the plate area having simple condition in longitudinal direction. And the coefficients c and d, which are the specific values for each case, can be defined as the proportional value to the column width b for each case. Which means

that those terms included in integration sign have constant value for every specific condition. Let modify these coefficients a, c and d to the coefficients proportional to b as $\alpha b(=a)$, $\gamma b(=c)$ and $\chi b(=d)$. Also, p_0 can be transformed to P/ac, and it can be written as $Pb^2/\alpha\gamma$ where P is external load. Then we can rewrite Eq. 21 and 22 as follows

$$w_1\left(\frac{a}{2},0\right)=\frac{P}{D}\cdot\frac{16}{\pi^6}\cdot\frac{b^2}{\gamma\chi}\sum_{m=1,3..}^{\infty}\sum_{n=1,3..}^{\infty}\frac{sin(\frac{\gamma}{\alpha}\cdot\frac{m\pi}{2})\cdot sin(\chi\cdot\frac{n\pi}{2})}{mn\left[\left(m^2/a^2\right)+\left(n^2/b^2\right)\right]^2} \quad (3.2.26)$$

$$\begin{aligned} w_2\left(\frac{a}{2},0\right)=&\frac{P}{D}\cdot\frac{8}{\pi^5}\cdot\frac{b^2}{\gamma\chi}\\ &\times\sum_{m=1,3..}^{\infty}\sum_{n=1,3..}^{\infty}\frac{tanh\left(\frac{1}{\alpha}\cdot\frac{m\pi}{2}\right)\cdot sin\left(\frac{\gamma}{\alpha}\cdot\frac{m\pi}{2}\right)\cdot sin\left(\frac{n\pi}{2}\right)\cdot sin\left(\chi\cdot\frac{n\pi}{2}\right)}{m\cdot cosh\left(\frac{1}{\alpha}\cdot\frac{m\pi}{2}\right)\cdot\left[\left(m^2/a^2\right)+\left(m^2/a^2\right)\right]^2}\\ &\times\frac{1}{\left[tanh\left(\frac{1}{\alpha}\cdot\frac{m\pi}{2}\right)\left(\left(\frac{1}{\alpha}\cdot\frac{m\pi}{2}\right)tanh\left(\frac{1}{\alpha}\cdot\frac{m\pi}{2}\right)-1\right)-\left(\frac{1}{\alpha}\cdot\frac{m\pi}{2}\right)\right]} \end{aligned} \quad (3.2.27)$$

From the Eq.3.2.26 and Eq.3.2.27, we can see that the terms included in integration sign is only α, γ and χ. Which means that complex equations included in integration sign can be presented in single coefficient if the proportional ratio α, γ and χ is fixed. The coefficients α would be determined as fixed value at Chapter 4 with numerical analysis using computer program Abaqus and the γ and χ is the specific value for each case, therefore, all the terms about α, γ and δ in the integration sign of Eq.3.2.26 and

Eq.3.2.27 can be expressed as κ_1 and κ_2, respectively after calculation of integration. Then Eq.3.2.26 and Eq.3.2.27 can be simplified with those coefficients, κ_1 and κ_2, and the other independent coefficients such as P, b and D as follow:

$$w_1 = \kappa_1 \cdot \frac{Pb^2}{D} \tag{3.2.27}$$

$$w_2 = \kappa_2 \cdot \frac{Pb^2}{D} \tag{3.2.28}$$

Substituting Eq. 3.2.27 and Eq.3.2.28 into Eq.3.2.22, the deformation of the center of the plate we assumed can be expressed as follow:

$$w_{p.max} = w_1 + w_2 = \left(\kappa_1 + \kappa_2\right) \cdot \frac{Pb^2}{D} \tag{3.2.29}$$

Chapter 4. Numerical Analysis for the Tension Strength of CFT Column

In previous theoretical Equation such as Eq.3.2.23 and Eq.3.2.24, variables such as b ,c and d are given condition, however, the variable a, the longitudinal length of virtual plate, has not been given and needed to be determined through experimental test or Numerical analysis. In this chapter, the numerical analysis model using computer program Abaqus having the similar condition as the theoretical equation would be proposed for obtaining the maximum displacement of the plate. And next, the variable a would be obtained as the proportional ratio α with the comparison between the theoretical equation and the numerical analysis results. In addition to this, modification factor Ψ would be applied through numerical analysis comparison between the bolt area and assumed area because actual loaded area is consisting of bolt area which is different from the assumed area. After these verification of theoretical equation, this model would be applied to numerical analysis and compared to experimental data having actual deformed shape as Fig.3.1.3. With these procedures, simplified equation for tension strength of the plate would be offered with the table containing coefficients for various load condition.

4.1 Completion of the theoretical equation

4.1.1 Finite element Strategy

The adopted finite element program, Abaqus, enables the material and geometric non-linearity to be taken into account. The finite element mesh used to model the CFT column is represented in Fig.4.1.1. For simplification, the finite element model was designed as the tubular steel section. To present the effect of concrete inside of tubular steel section, inside plate of the tubular section except the loaded plate is fixed in x, y, z direction. The other boundary conditions were: all base nodes fixed in x, y, z direction, one base node full fixed and another, in opposite side have same manner. In case of load condition, the 1kN of load was distributed to the area surrounded by c and d for assumed loaded area as Fig.3.1.2. and by square of c for representing bolt area.

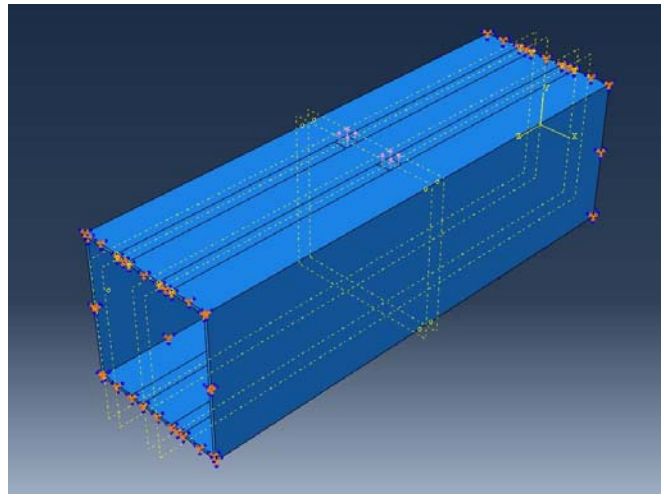

Fig. 4.1.1 Finite element modeling

4.1.2 Abaqus Set-up

The tubular section having the length of 1m had been used for the numerical analysis to represent the whole CFT column. The other tubular section having length of 500mm, 700mm, 1500mm had been considered, however, in the case of 500mm and 700mm model were lack of its length to present the stresses induced by the force and in the case of 1500mm model was redundant due to the finite element model's fixed boundary condition. Thus, the model of the tubular section having length of 1m had been chosen.

The parameters for composing Abaqus modeling are as follow: The deformable type and solid elements were used to model the plate of the column for numerical analysis based on the plate theory. And 200 GPa and 0.3 pf poisson's ratio, static model, independent instance type were adopted for this numerical model.

The magnitude of meshes are determined depend on the size of numerical analysis models. In this paper, the tubular square sections having the width of 150mm, 200mm and 300mm are examined. For 150mm and 200mm model, 2mm square mesh were used, and for 30mm model, 3mm square mesh were used to modify the variance due to the size.

4.1.3 Dimension of Abaqus models

Five Abaqus models were undertaken to compare these data to the theoretical equation using the plate theory. As we discussed before, theoretical equations for CFT column's plate to tension load is obtained as Eq.3.2.23 and Eq.3.2.24. And these

equations coefficients have variables such as P, b and D, and coefficients including α, γ and χ. Unlike given condition such as c, longitudinal length of loaded area, and d, transverse length of loaded area, a is needed to be determined through comparison with numerical analysis and theoretical equation. For this comparison, five sets of tubular column having length of 1m and various dimensions such as loaded area, column' thickness and width are established as Fig.4.1.2 and table 4.1.1.

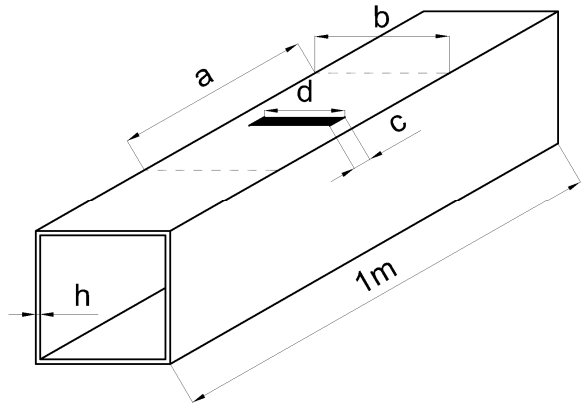

Fig. 4.1.2 Numerical Analysis Model

Table 4.1.1 Dimension of Numerical Analysis Model

	b	c(γ)	d(χ)	h
Case #1	150	8.8(0.058)	53.8(0.358)	6.3
Case #2	150	8.8(0.058)	53.8(0.358)	10
Case #3	200	16(0.08)	72(0.36)	10
Case #4	200	80(0.4)	120(0.6)	10
Case #5	300	80(0.4)	150(0.5)	10

To consider various condition of CFT column, each case has different value of α, γ, χ and b. We can observe the effect of column depth(h) with the comparison between case #1 and the case # 2, and the effect of loaded area(c & d) with the comparison between case #3 and the case # 4. Also, proposed equation can be verified for different column width(b) through case #1, #3 and #5.

For each case, proposed equation has only one variable "a" due to b, c, d and h is given. Thus, the assumed length a can be obtained through comparing this equation to the numerical analysis result. These result is shown from Fig 4.1.3 to Fig.4.1.7

4.1.4 Determining coefficient a

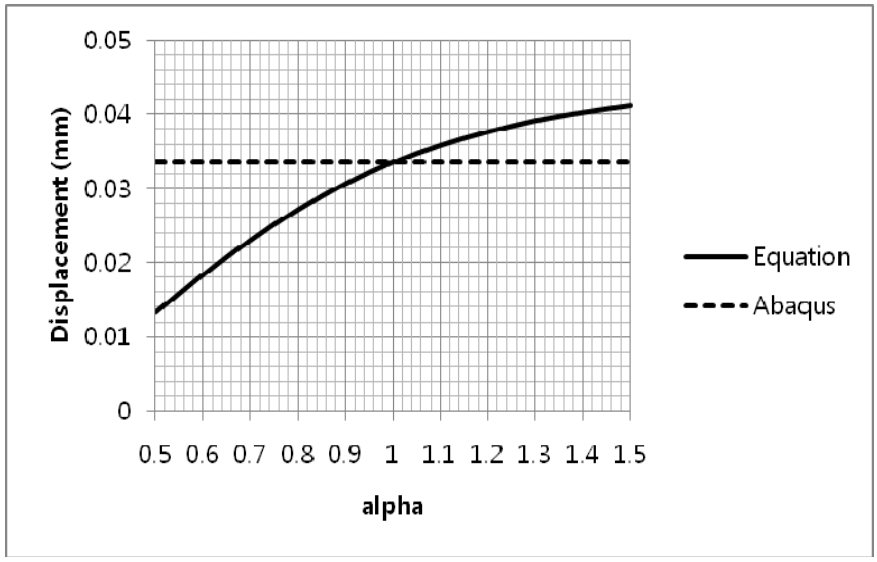

Fig. 4.1.3 Result(displacement) comparison between proposed equation and numerical analysis for case #1

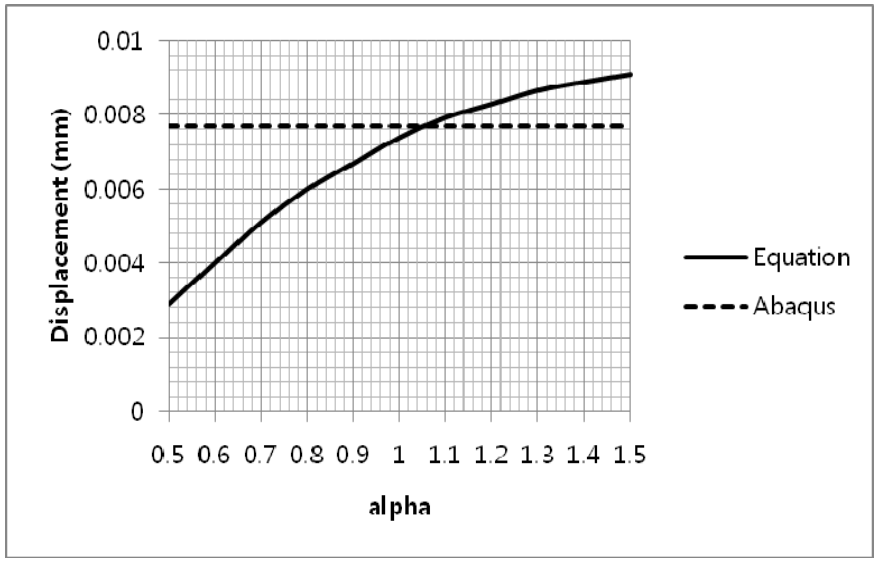

Fig. 4.1.4 Result(displacement) comparison between proposed equation and numerical analysis for case #2

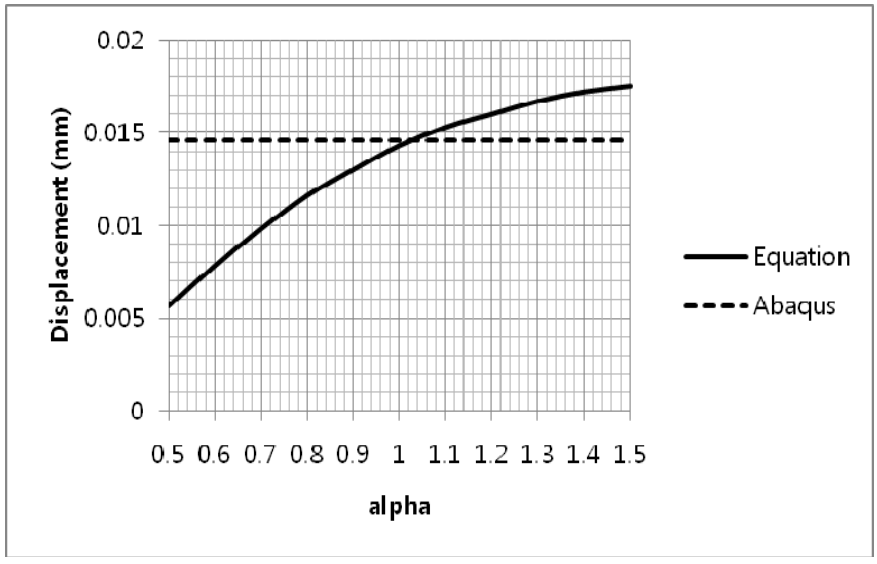

Fig. 4.1.5 Result(displacement) comparison between proposed equation and numerical analysis for case #3

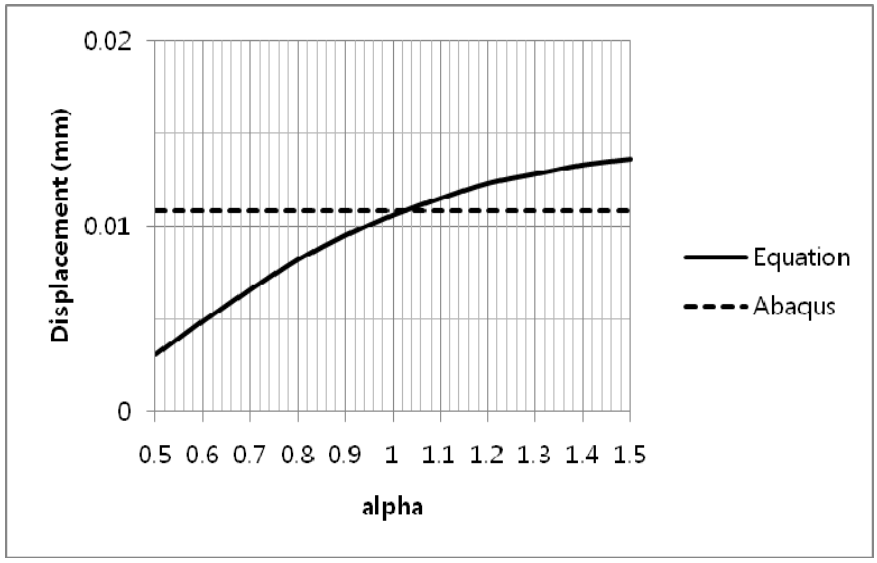

Fig. 4.1.6 Result(displacement) comparison between proposed equation and numerical analysis for case #4

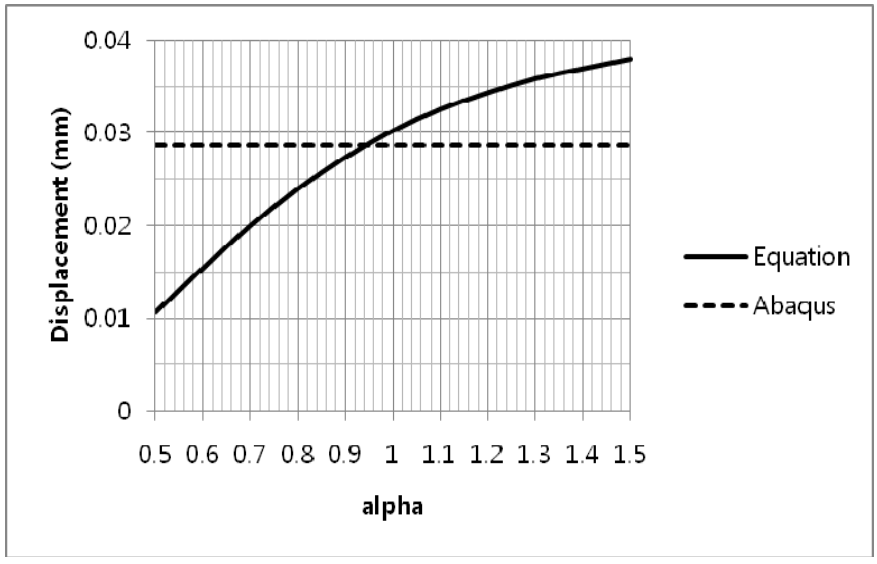

Fig. 4.1.7 Result(displacement) comparison between proposed equation and numerical analysis for case #5

Table 4.1.2 Deformation Results Comparison between proposed equation and numerical analysis

	Numerical analysis	Theoretical Equation. (when α=1.0)	Relative error
Case 1	0.0335mm	0.0336mm	0.3%
Case 2	0.0077mm	0.0074mm	-4.0%
Case 3	0.0146mm	0.0143mm	-2.1%
Case 4	0.0108mm	0.0106mm	0.9%
Case 5	0.0287mm	0.0302mm	4.9%

As indicated from Fig.4.1.3 to Fig 4.1.7, proposed equation is well fitted when α, the proportional ratio a to b, is about 0.8 with relative error up to 4.9%, and this results is shown at table 4.1.2. Thus, the value of α is verified as 1 for the maximum deflection of the CFT column's plate.

4.2 Modification factor for assumed loaded area

So far, we assumed the loaded area, c times d, as rectangular area for convenience to apply the plate theory as indicated in fig 4.1.1(a). However, the actual loaded are is bolt area which is different from assumed area as indicated in fig 4.1.1(b). Therefore, the modification factor is needed to fit the actual model.

To obtain the modification factor, we need to set the numerical analysis model having the actual loaded area (bolt area) as Fig.4.1.1(b) and compare this model to assumed model as Fig.4.1.1(a). These models are also established with just same

strategy and boundary condition as the model dealt in Chapter 4.1, which is evaluated by tension experiments in Chapter 4.2. The load is pressured as the total amount of 1kN for both case, and the pressure for each case is divided with each loaded area. For example, In case of case #1, 0.00211GPa (1/(assumed area=8.8*53.8)) is pressured for assumed rectangular area and 0.00645GPa (1/(bolt area=8.8*8.8*2)) is pressured for blot area.

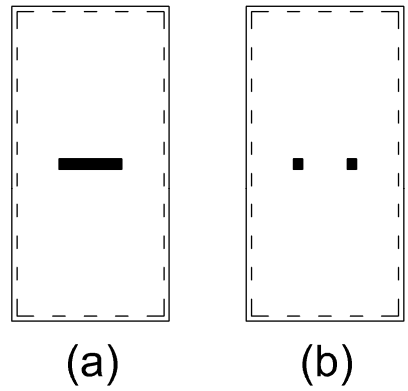

Fig. 4.2.1 Loaded area: (a) assumed area (b) actual bolt area

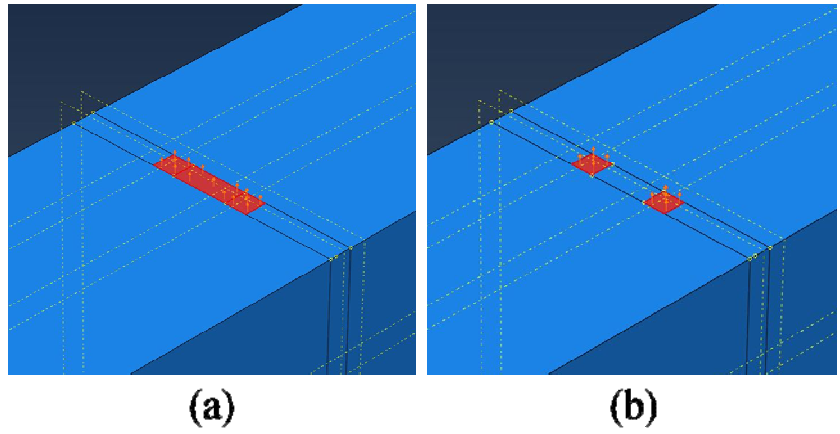

Fig. 4.2.2 Loaded area in Aqaqus: (a) assumed area (b) bolt area

To compare these values, five sets of numerical analysis model had been considered just same as table 4.1.1. From case#1 to case#3, their loaded area indicate the single row of bolt configuration, case#4 and case#5 indicate the double row of that. In case of model for actual bolt area, d of table 4.1.1 had been altered to express bolt area. These results area indicated in table 4.2.1, Fig 4.3.9 and Fig.4.3.10.

By numerical analysis, our assumption has the relative error about 20% for single bolt row(case#1, #2 and #3) and 40% for double bolt row(case#4 and #5) as indicated at table 4.2.1. Due to the alteration of loading point and area, overall behavior is quite different from each other shown as Fig.4.2.3 and Fig 4.2.4. However, we can still assume that both case have something in common such as deflection shape and stress distribution as we assumed. Thus, we can obtain the tension strength of the CFT column's plate with modification factor.

Table 4.2.1 Numerical analysis results: Assumed area versus actual area

	Assumed area	Actual(bolt) area.	Relative error
Case 1	0.0335mm	0.0287mm	16.7%
Case 2	0.0077mm	0.0064mm	20.3%
Case 3	0.0146mm	0.0127mm	14.9%
Case 4	0.0108mm	0.0065mm	39.4%
Case 5	0.0301mm	0.0211mm	42%

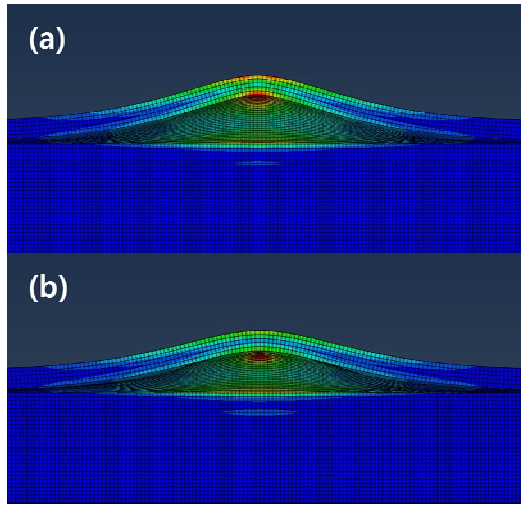

Fig. 4.2.3 Abaqus data comparison: (a) assumed area (b) bolt area

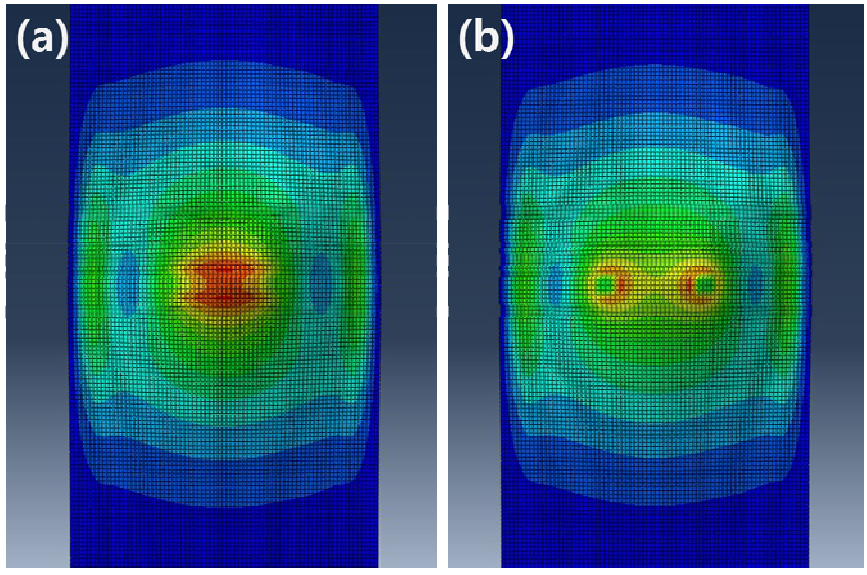

Fig. 4.2.4 Abaqus data comparison: (a) assumed area (b) bolt area

4.3 End-plate effect

4.3.1 Theoretical equation considering end-plate effect

From chapter 4.1 to chapter 4.2, the maximum tension deflection equation of the plate having the boundary of CFT column condition had been derived. However, to obtain the actual stiffness of the plate with end plate or angle, central deformation signifies nothing because the deformation geometry is changed as indicated at Fig.3.1.3. As Fig.3.1.3, the portion of the plate between the bolts is not changed vertically or horizontally, thus, we can assume the maximum deformation of this plate is presented at the boundary of assumed loaded area as illustrated in Fig.4.3.1.

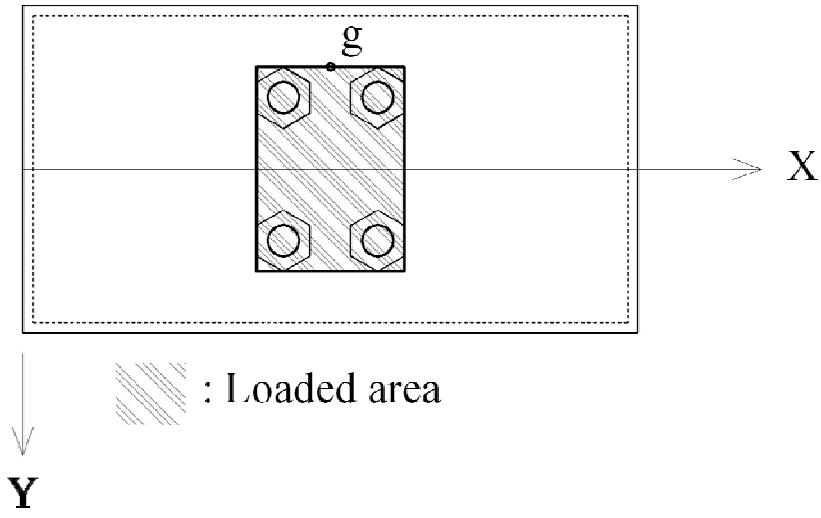

Fig. 4.3.1 The boundary of the loaded area and measuring point g

Therefore, the deformation of the plate having the geometry as Fig.3.1.3 had been measured at point g of Fig.4.3.1 having the coordinate x=d/2 and y=a/2. Substituting this coordinate into Eq.3.2.16 and Eq.3.2.21, the deformations of each action at the boundary of the loaded plate can be obtained as follwing: and sum of these equation is the deformation of the plate of CFT column with end plate or angle.

$$w_1\left(\frac{a}{2},\frac{d}{2}\right)=\frac{16p_0}{D\pi^6}\sum_{m=1}^{\infty}\sum_{n=1}^{\infty}\frac{\left[sin\left(\frac{m\pi}{2}\right)\right]^2\cdot sin\left(\frac{n\pi}{2}\right)}{mn\left[\left(m^2/a^2\right)+\left(n^2/b^2\right)\right]^2}$$
$$\times sin\left(\frac{c}{a}\cdot\frac{m\pi}{2}\right)\cdot sin\left(\frac{d}{b}\cdot\frac{n\pi}{2}\right)\cdot sin\left(\frac{n\pi}{2}\cdot\left(\frac{d}{b}+1\right)\right) \tag{4.3.1}$$

$$w_2\left(\frac{a}{2},\frac{d}{2}\right)=\frac{8p_0}{\pi^5 D}\sum_{m=1}^{\infty}\sum_{n=1}^{\infty}\frac{\left[sin\left(\frac{m\pi}{2}\right)\right]^2\cdot sin\left(\frac{c}{a}\cdot\frac{m\pi}{2}\right)\cdot sin\left(\frac{n\pi}{2}\right)\cdot sin\left(\frac{d}{b}\cdot\frac{n\pi}{2}\right)}{m\cdot\left[\left(m^2/a^2\right)+\left(m^2/a^2\right)\right]^2}$$
$$\times\frac{\left[tanh\left(\alpha_m\right)\cdot cosh\left(\frac{d}{a}\cdot\frac{m\pi}{2}\right)-\frac{d}{b}sinh\left(\frac{d}{a}\cdot\frac{m\pi}{2}\right)\right]}{cosh\,\alpha_m\cdot\left[tanh\,\alpha_m\left(\alpha_m\,tanh\,\alpha_m-1\right)-\alpha_m\right]} \tag{4.3.2}$$

And sum of these equation is the deformation of the plate of CFT column with end plate or angle.

$$w_{p.CFT} = w_1 + w_2 \tag{4.3.3}$$

With the same procedure of chapter 3.2.3, the coefficients a, c and d in Eq.4.3.1 and Eq.4.3.2, which are the dimension of assumed length and loaded area, can be represented to α, γ and χ as following:

$$w_1\left(\frac{a}{2},\frac{d}{2}\right) = \frac{Pb^2}{D}\cdot\frac{16}{\chi\cdot\gamma\cdot\pi^6}\sum_{m=1,3..}^{\infty}\sum_{n=1,3..}^{\infty}\frac{\left[sin\left(\frac{m\pi}{2}\right)\right]^2\cdot sin\left(\frac{n\pi}{2}\right)}{mn\left[\frac{1}{\alpha^2}m^2+n^2\right]^2} \times sin\left(\frac{\gamma}{\alpha}\cdot\frac{m\pi}{2}\right)\cdot sin\left(\chi\cdot\frac{n\pi}{2}\right)\cdot sin\left((\chi+1)\cdot\frac{n\pi}{2}\right) \tag{4.3.4}$$

$$w_2\left(\frac{a}{2},\frac{d}{2}\right) = \frac{Pb^2}{D}\cdot\frac{8}{\chi\cdot\gamma\cdot\pi^5}\sum_{m=1}^{\infty}\sum_{n=1}^{\infty}\frac{\left[sin\left(\frac{m\pi}{2}\right)\right]^2\cdot sin\left(\frac{n\pi}{2}\right)\cdot sin\left(\frac{\gamma}{\alpha}\cdot\frac{m\pi}{2}\right)}{m\cdot cosh\left(\frac{1}{\alpha}\cdot\frac{m\pi}{2}\right)\cdot\left[\frac{1}{\alpha^2}m^2+n^2\right]^2} \times\frac{sin\left(\chi\cdot\frac{n\pi}{2}\right)\cdot\left[tanh\left(\frac{1}{\alpha}\cdot\frac{m\pi}{2}\right)\cdot cosh\left(\frac{\chi}{\alpha}\cdot\frac{m\pi}{2}\right)-\chi\cdot sinh\left(\frac{\chi}{\alpha}\cdot\frac{m\pi}{2}\right)\right]}{\left[tanh\left(\frac{1}{\alpha}\cdot\frac{m\pi}{2}\right)\left(\left(\frac{1}{\alpha}\cdot\frac{m\pi}{2}\right)tanh\left(\frac{1}{\alpha}\cdot\frac{m\pi}{2}\right)-1\right)-\left(\frac{1}{\alpha}\cdot\frac{m\pi}{2}\right)\right]} \tag{4.3.5}$$

And as mentioned above, all the terms about α, β and χ in Eq.3.2.25 and Eq.3.2.26

can be expressed as κ_1 and κ_2, respectively, after calculation of integration. Thus, Eq.4.3.4 and Eq.4.3.5 can be simplified with these coefficients, κ_1 and κ_2, and sum of these equation should be the deformation of the plate at the boundary of loaded area as follow:

$$w_{p,CFT} = w_1 + w_2 = (\kappa_1 + \kappa_2) \cdot \frac{Pb^2}{D} \tag{4.3.6}$$

Then the tension stiffness of the plate in CFT column at the center of load can be written as:

$$\begin{aligned} P &= \frac{D}{b^2} \cdot \frac{1}{(\kappa_1 + \kappa_2)} w \\ k_{p.CFT} &= \frac{D}{b^2} \cdot \frac{1}{(\kappa_1 + \kappa_2)} \end{aligned} \tag{4.3.7}$$

4.3.2 Numerical analysis model for end plate effect

The value α of Eq.4.3.4 and Eq.4.3.5 need to be redefined even though it had been derived by the numerical analysis in chapter 4.1. That's because the boundary condition and the measuring point was changed. Thus, the new numerical analysis model for the geometry of Fig.3.1.3 had been developed and represented at Fig.4.3.2.

To present the end plate effect, this numerical analysis model adopted following factors in addition to numerical strategy of chapter 4.1:

First, the stiffness of loaded plate was set to infinite to keep this area from deforming vertically or horizontally. Second, this model adopted the plate shape instead of tube shape. Third, all of the side face of the plate is fixed in x, y, z direction to present the effect of concrete inside of tubular steel section as boundary condition.

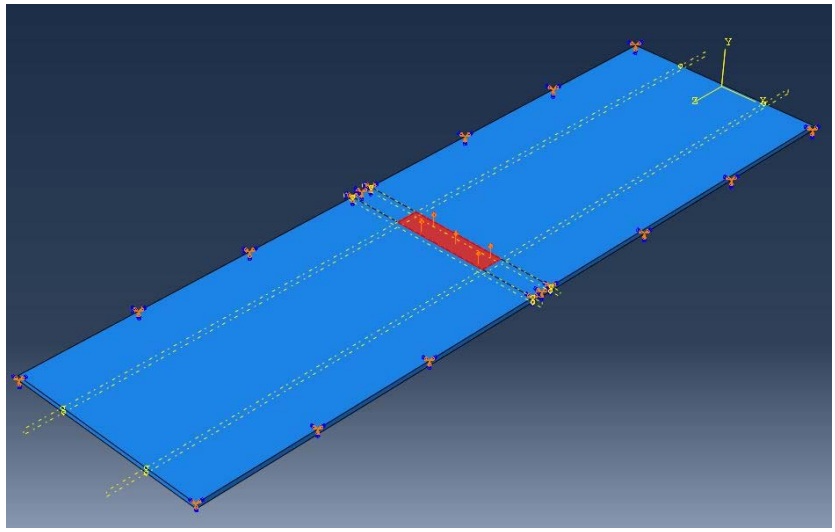

Fig. 4.3.2 Finite element modeling

To verify the reliability of this numerical analysis model by the experiments, four set of Abaqus model had be designed with the same dimension of specimens as table 4.2.1.

4.3.3 Test set-up and parameters

The finite element analyses of the tested specimens were carried out to check the validity of the finite-element model. Fig.4.2.1 shows that the tested geometries and table 4.2.1 gives a general overview of the six static monotonic tests that were performed:

two (E13, E14) connecting an IPE 240 beam to a RHS 200*6 column by an extended end plate with one bolt row in the extended part of the plate - type (a) configuration, and two other (E16, E17) with similar geometry. These two geometries were tested under positive and negative moments. On type (c) configuration (flush end plate), two further test (E19, E21) were performed where an IPE 300 beam is connected to a SHS column (with 6mm or 16mm thickness).

All the tests used studs welded to the column face in the fabrication shop and the beam end plate was machined to accommodate the welds. With the system, there is no projection of the connection elements to the inside of the column, and therefore no interaction with the infilling concrete occur. This is particularly suitable in the current analysis as its objective is to isolate the behavior of the column face. Previous tests with the same system conducted by Maquoi et al. (1983) presented rotations ranging from 70 mrad up to 120 mrad while other tests conducted by Vandegans (1995) achieved a minimum value of 50mrad. However, in the present study, the joint ductility is clearly limited by the stud-face connection. As the failure is in the connecting weld itself, this limitation should be solved by more accurate technological procedures in the fabrication shop.

Table 4.3.1 Dimension of Experiment Model

Teet	γ	χ	h
E13	0.54	0.13	6mm
E16	0.54	0.49	6mm
E19	0.45	0.1	6mm
E21	0.45	0.1	16mm

Table 4.3.2 Strength and joint type of Experiment Model

Teet	Column	Steel	Beam	Steel	Type
E13	SHS 200*6	S 355	IPE 240	S 275	one bolt row in tension
E16	SHS 200*6	S 355	IPE 240	S 275	two bolt rows in tension
E19	SHS 300*6	S 355	IPE 300	S 275	Flush
E21	SHS 300*16	S 355	IPE 300	S 275	Flush

Fig.4.2.1 illustrates the test layout together with the loading frame and specimens. The column base was supported by the hinge fixed to a cast in place reinforced concrete foundation and at the top, the column was fixed with a device shown in Fig.4.2.1. The load was applied through a hydraulic jack with 200kN capacity and a 200mm stoke. With the adopted test setup it would be possible to achieve rotations of about 200mrad in these monotonic tests, Neves et al. (2003). No axial force applied in the column, as the main objective was to characterize the column face under out-of-plane bending.

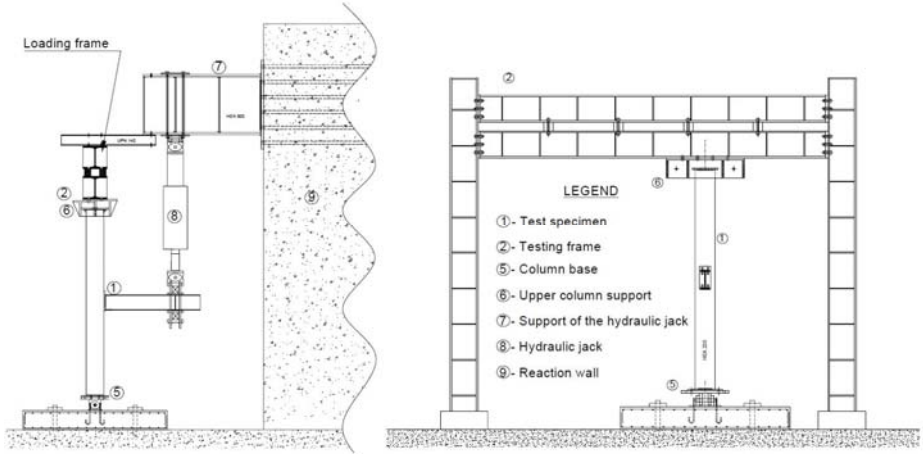

Fig. 4.3.3 Test layout (Neves 1996; Silva et al.2003)

The end plate, a much stiffer and resistant component when compared to the column face had a negligible deformation and remained in the elastic range for the negative moment tests. The column face had been overstrengthened due to membrane action led to the welded stud failures. This fact occurred for moments exceeding between 1.7 and 3.0 times the level of moment corresponding to the change of the slope in the $M-\varphi$ curve (except in Test E21 where the International Journal of Applied Mechanics and Engineering 10/16 failure occurred in the component elastic range). These welded studs collapsed with the tearing of the welds on the stud surface, while the measured internal stud stresses were still in the elastic range. These measurements allow the derivation of the force-displacement ($F - \Delta$) curves of the column face, combined with the displacement measurements in Fig.4.2.2. In the present study, this information is used to calibrate a model to derive the $F - \Delta$ curves from the externally applied bending moments.

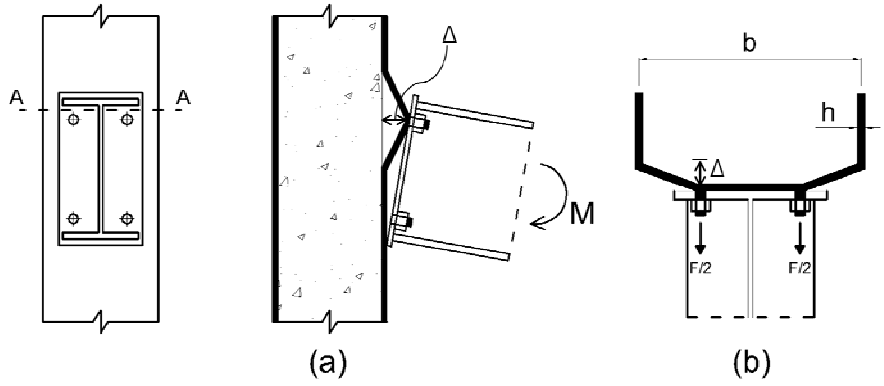

Fig. 4.3.4 Relevant geometrical characteristics of the joint (Neves 1996; Silva et al.2003) (a): Typical behavior of the column loaded face, (b) Typical behavior of the column loaded face at A-A section

4.3.4 Result comparison

The comparison between the Abaqus results and experimental data had been represented from Fig.4.3.5 to Fig.4.3.8.

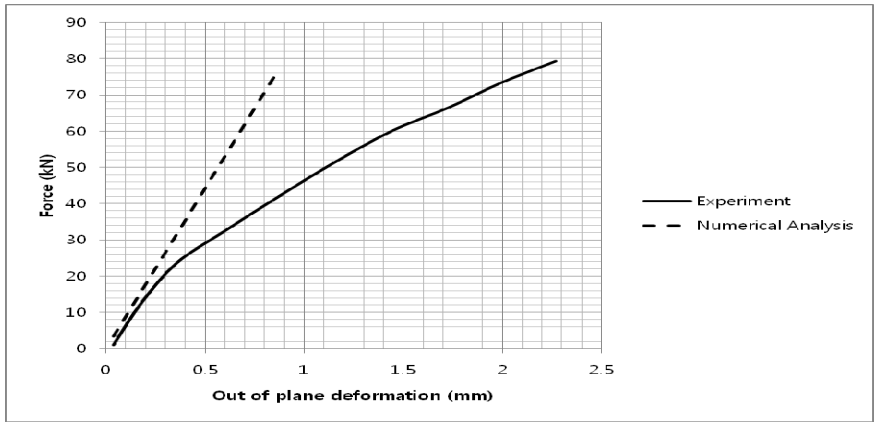

Fig. 4.3.5 Result(displacement) comparison between experiment and numerical analysis for case E13

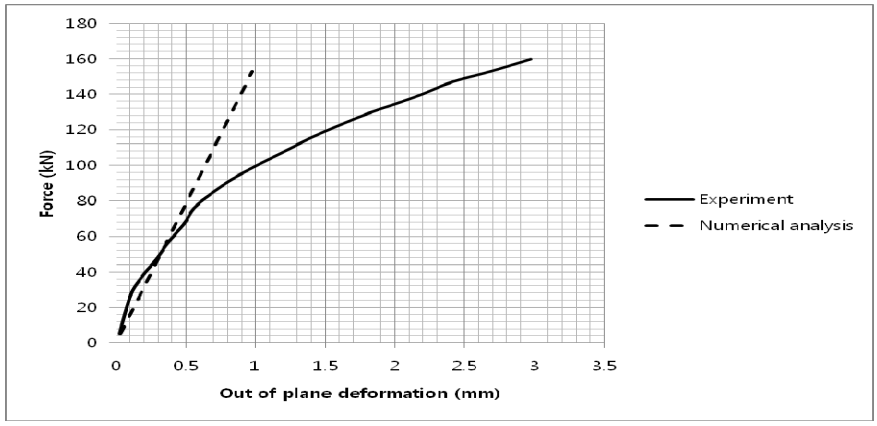

Fig. 4.3.5 Result(displacement) comparison between experiment and numerical analysis for case E16

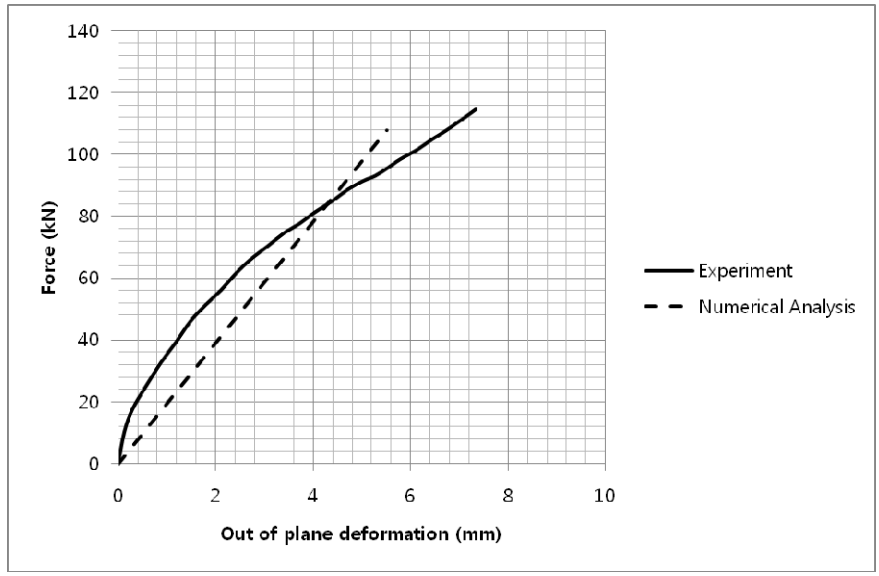

Fig. 4.3.5 Result(displacement) comparison between experiment and numerical analysis for case E19

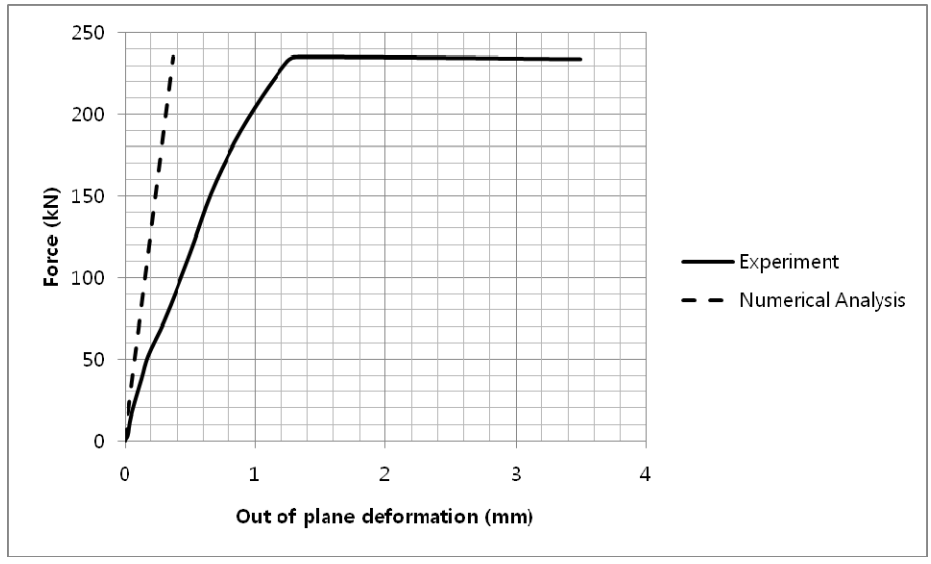

Fig. 4.3.5 Result(displacement) comparison between experiment and numerical analysis for case E21

As shown at above comparison graphs, the reliability of the numerical analysis modeling for the plate having end plate effect had been testified successfully. Therefore, the value α for the plate containing the end-plate effect can be determined with these data and modification factor obtained at chapter 4.2. With the procedure of chapter 4.1.4, the value α had been determined as 0.7, and the result had been shown at table 4.3.3

Table 4.3.3 Numerical analysis results comparing to theoretical equation

	Numerical Analysis	Theoretical Equation (α=0.7) With modification factor	Relative error
E13	1.13mm	1.2mm	6%
E16	0.64mm	0.69mm	7%
E19	5.12mm	4.416mm	-16%
E21	0.156mm	0.163mm	4%

4.4 The equation for tension stiffness of the CFT column

Proposed equation is still too complex to use due to complicate terms in sigma even though we obtained exact value of α, proportional ratio assumed length for simple supported to column width. However, this equation can be simplified on the fact that it is composed of the proportional ratio. In proposed equation of Eq.4.3.4 and Eq.4.3.5, all the terms except P, D and b are the proportional ratio to b. In case of a, proportional ratio of a to b, this variable had been defined in chapter 4.3 as 07. For the left variables such as γ and χ, is the given condition for specific loading case. Because these terms are proportional ratio, the proposed equation have the same stiffness without reference to

load, column width or thickness if the proportional ratio to b is same. Therefore, these equations can be simplified as number for each loading case having same proportion to b. With these procedure the coefficient of κ_1 and κ_2 in Eq.4.3.6 can be defined, then the tension stiffness of CFT plate, $k_{T,plate.c}$, can be obtained. If we let the coefficient $1/(\kappa_1 + \kappa_2)$ of Equation 4.3.7 as κ , this equation can written as:

$$k_{p,CFT} = \kappa \cdot \frac{D}{b^2} \tag{4.4.1}$$

Table 4.4.1 The coefficient of the tension stiffness of CFT column plate for each loading case having same proportion ratio to column width b

χ \ γ	0.05	0.1	0.2	0.3
0.3	246.7	249	257.8	272.2
0.4	306.9	309.7	320.5	338.2
0.5	403.6	407.3	421.8	445.4
0.6	573.5	579	600.4	635

And the results of calculation for this coefficient κ for each loading case having same proportion to b are shown at table 4.4.1.

The coefficients κ in table 4.4.1 are varies from 143.5 to 214.7. Even though the same load is applied in to each case, the stiffness is getting bigger as the loaded area is more huge and smaller as the loaded area is smaller. For more accurate coefficient, we need to consider the difference between the assumption and actual case dealt in chapter 4.2.3. Thus, the governing equation for the tension stiffness of CFT column can be

written as follow.

$$k_{p,CFT,e} = \psi \cdot \kappa \cdot \frac{D}{b^2} \tag{4.4.2}$$

where Ψ is modification factor, κ is loaded area coefficients, b is the CFT column width and D is $Eh^3/(1+\nu^2)$.

To verify the reliability of the proposed equation, Eq.4.4.2, this had been compared with experimental data and numerical analysis result from Fig.4.4.1 to Fig.4.4.3 on the condition of table 4.2.1.

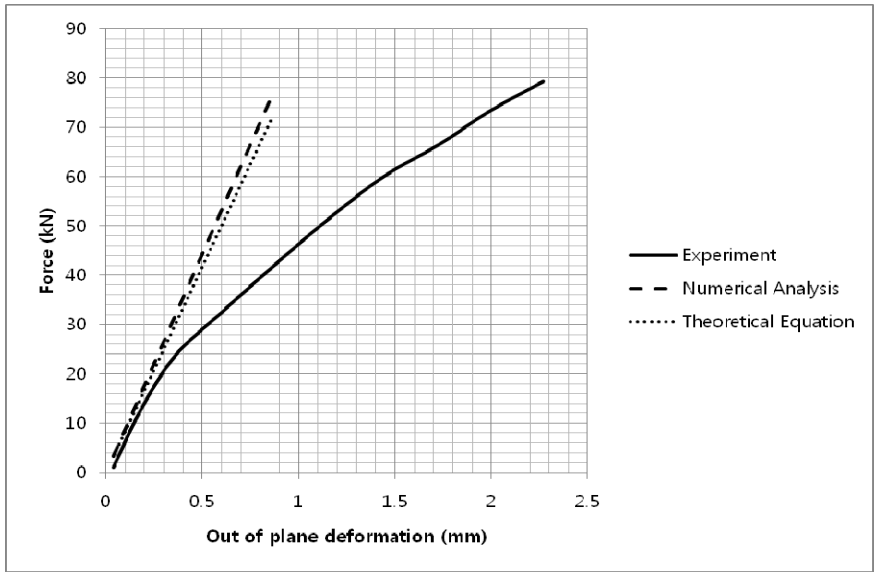

Fig. 4.4.1 Result(displacement) comparison with proposed equation, experimental data, numerical analysis for case E13

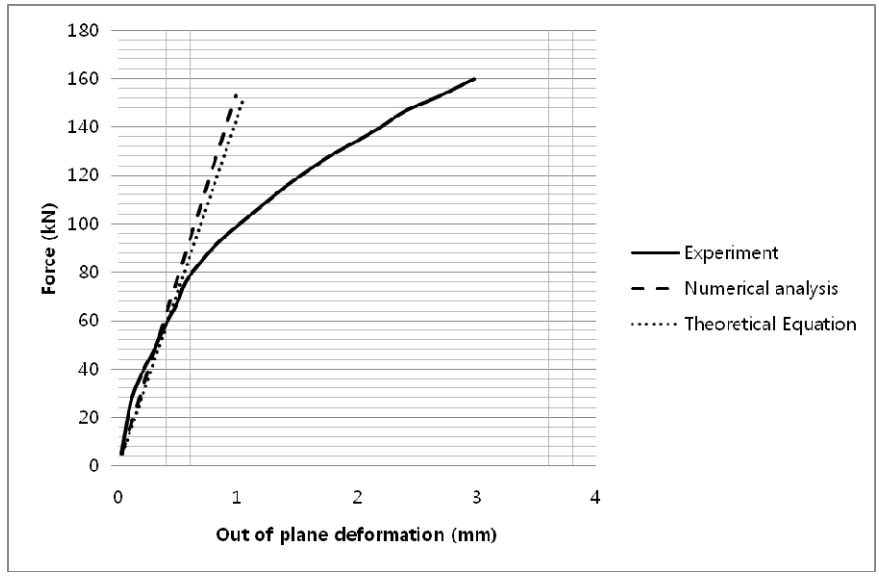

Fig. 4.4.2 Result(displacement) comparison with proposed equation, experimental data, numerical analysis for case E16

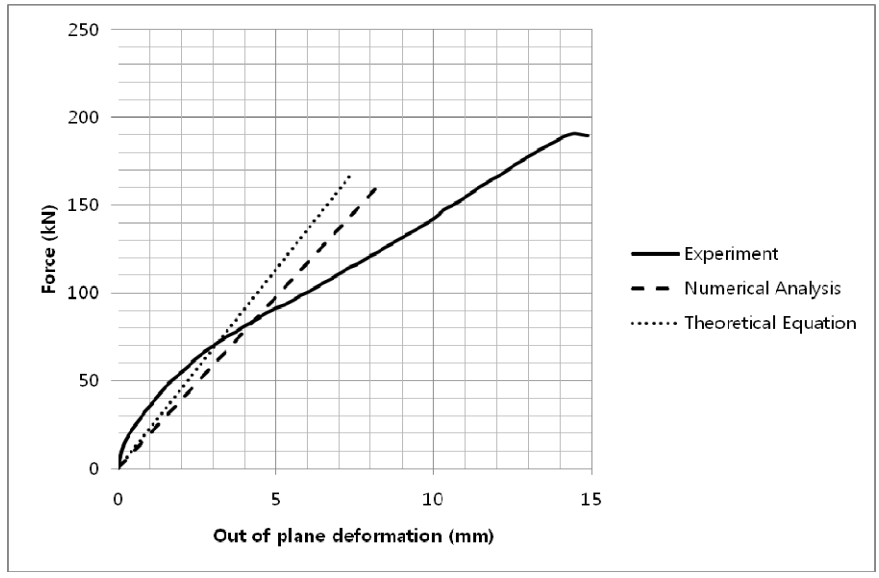

Fig. 4.4.3 Result(displacement) comparison with proposed equation, experimental data, numerical analysis for case E19

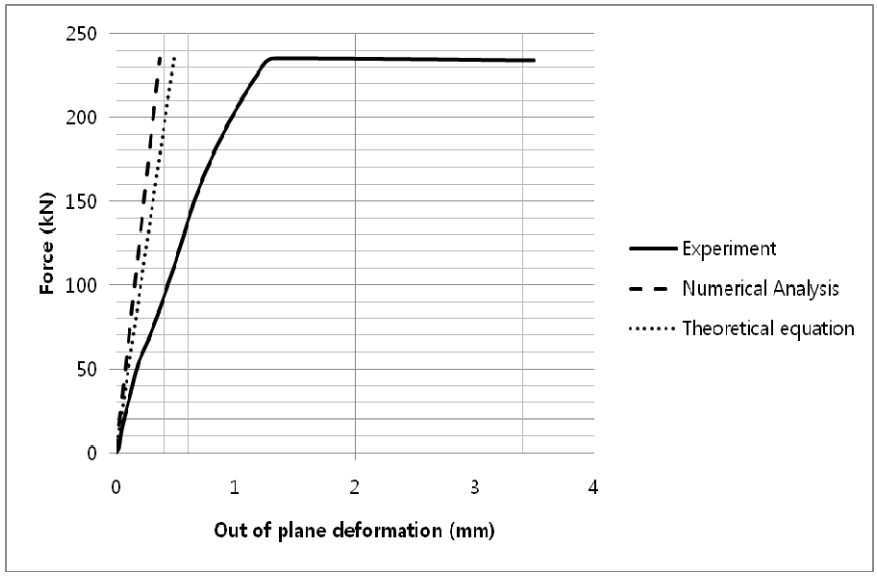

Fig. 4.4.4 Result(displacement) comparison with proposed equation, experimental data, numerical analysis for case E21

To apply Eq.4.4.2 to specific case having two decimals such as χ=0.35, median value of κ when χ=0.3 and χ=0.4 can be adopted.

As result shown, the proposed equation is well compatible not only to experimental data but also to numerical analysis. Thus, this equation can be used as the tension stiffness of CFT column's plate for the component method.

Chapter 5. The Application of the Proposed Equation to the Component Method

5.1 The example of semi-rigid connection

To apply the proposed equation for the tension stiffness of the CFT column, the example of the semi-rigid joint having bolt connection and end plate arranged as Fig.5.1.1.

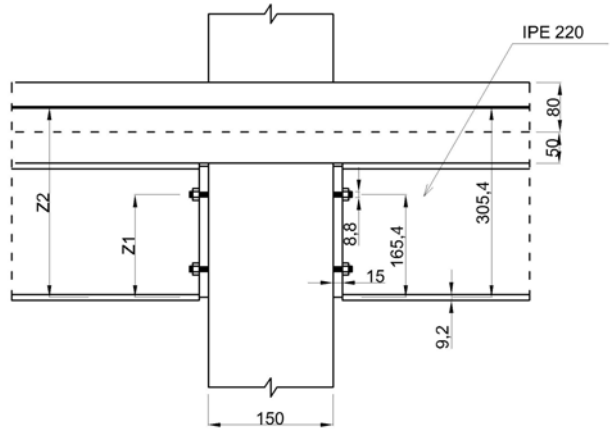

Fig. 5.1.1 Semi-rigid connection with CFT column on transverse view

The dimension of this semi rigid joint is shown at Fig.5.4.1 and Fig.5.4.2. The other material properties are as follow: IPE 220 is used for transverse beam and grade S235 steel was used all steel components. Concrete has the 20MPa of the strength and

29000Mpa of young's modulus. Connector has the 100kN/mm of stiffness and located with 100mm space. The detail of this example and calculation of the characteristics of component can be obtained Eurocode's worked example - Stiffness and resistance calcaulation for beam-to-column composite joints with flush end-plates. In this example, only H-beam column section had been changed to CFT column section.

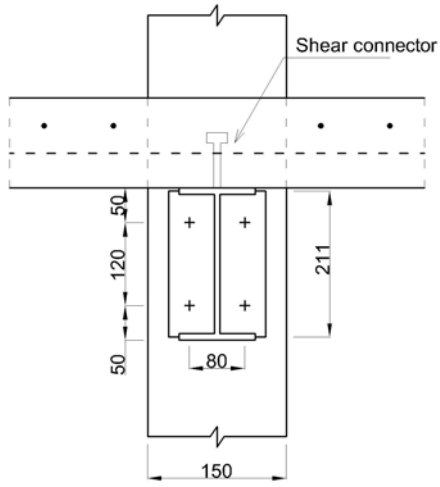

Fig. 5.1.2 Semi-rigid connection with CFT column on longitudinal view

5.2 The component identification

The component identification is regarding the joint as an assembly of a separate element of finite size, and dividing each element composing connection into compression, tension and shear zone. In case of the semi-rigid joint as shown in Fig.5.1.1, it can be divided into 8 components as shown in Fig.5.1.2 as following: (1) CFT column in shear, (2) CFT column in compression, (3) beam flange in compression,

(4) end plate in bending, (5) bolt row in tension, (6) beam web in tension and (7) column plate in tension(tension).

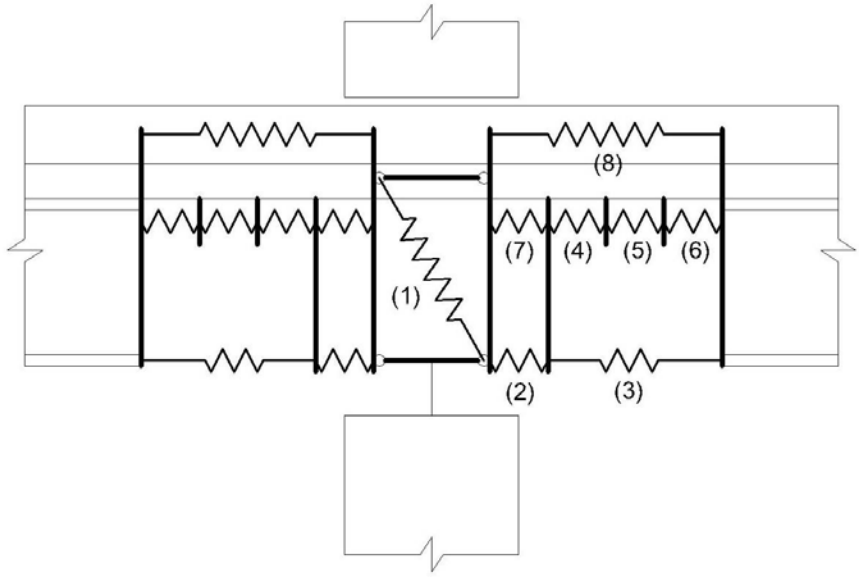

Fig. 5.2.1 Equivalent elastic system for the example

5.3 The component characteristics

The characteristics, the stiffness and the strength, of some components in Fig.5.1.2 had been well defined at EC3 such as (2) CFT column in compression, (3) beam flange in compression, (4) end plate in bending, (5) bolt row in tension and (6) beam flange in bending. Therefore, missing component's characteristics such as (4) the strength of the CFT column's plate and (1) the strength and the stiffness of the CFT column in shear would be dealt in this chapter.

5.3.1 The strength of the CFT column's plate

To earn the strength of the CFT column's plate, yield line theory, an ultimate load analysis, had been adopted. For the stiffness of the CFT column's plate, its equation had been derived from the plate theory. However, it cannot be applied to ear the strength of the strength because it deal only with the elastic region, thus, yield line theory covering the plastic region need to be applied to earn it. The yield line theory establishes either the moments in an element at the point of failure or the load at which an element will fail with using work method. The fundamental principle of work method is that work done internally and externally must balance as Eq.5.3.1.

$$\sum\left(N\times\delta\right)=\sum\left(m\times l\times\theta\right) \tag{5.3.1}$$

In Eq.5.3.1, the left term and the right term indicates the external load and the internal energy, respectively, where N is load acting within a particular region , χ is the vertical displacement of the loads N on each region expressed as a fraction of unity, m is the unit moment in or unit moment of resistance of the plate, l is the length of yield and θis the rotation of the region about its axis of rotation.

This theory can be applied to our assumed model having fixed boundary condition in transverse direction and simple boundary condition in longitudinal direction as illustrated in Fig.3.1.5(a), and yield line of this model can be represented with dotted line as Fig.5.3.1.

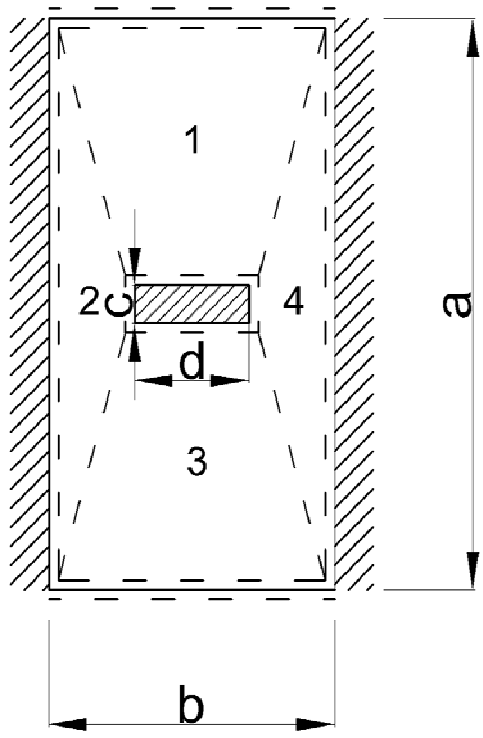

Fig. 5.3.1 Yield line for CFT column's plate under bolt loading

In this yield line model, external energy(E_E) due to distributed load, p_z, can be written as Eq.5.3.2 where P is total external load.

$$E_E = p_z \times c \times d \times \delta = P \times \delta \tag{5.3.2}$$

Internal energy can be earned dividing the plate into 4 sections surrounding yield line as indicated in Fig.5.3.1. In case of zone 1 and zone 3, yield line is formed only inside of the plate except the boundary. And the slope of the plate due to external load can be represented as the deflection and the distance from the boundary to the loaded

area in the assumption of small angle. Thus, the internal energy in zone 1 and zone 3 in Fig.5.3.1 can be written as Eq.5.3.3 where m is the unit moment in the plate.

$$E_{i1,3} = m \times b \times \frac{\delta}{(a-c)/2} \tag{5.3.3}$$

In case of zone 1 and zone , the yield line is formed both on the inside of the plate and the boundary. Thus, the internal energy in zone 1 and zone 3 in Fig.5.3.1 can be earned the sum of the unit moment in the plate(m) and the unit moment at the boundary(m') as indicated in Fig5.3.4.

$$E_{i2,4} = m \times a \times \frac{\delta}{(b-d)/2} + m' \times a \times \frac{\delta}{(b-d)/2} \tag{5.3.4}$$

Here, the assumed length a had been earned as 0.8b and m would be the same as m' at the plastic region. Because the sum of the internal energy should be the same as the sum of the external energy, Eqs.5.3.2, 5.3.3,5.3.4 can be written as follow.

$$P \times \delta = \left(\frac{2mb}{\left(\frac{a-c}{2}\right)} + \frac{4ma}{\left(\frac{b-d}{2}\right)} \right) \times \delta \tag{5.3.5}$$

$$P = \frac{4mb}{a-c} + \frac{8ma}{b-d}$$

Here, the length a is unknown length and can be calculated when yield line solution has minimum value because yield lines will always follow the path of least resistance (the length a is not the value of αb, calculated for the strength of the plate). Thus, the minimum value can be obtained by using the first derivative of Eq.5.3.5:

$$\frac{\partial P}{\partial a} = \frac{4mb}{(a-c)} + \frac{8m}{b-d} == 0 \tag{5.3.6}$$

$$a = \sqrt{\frac{b \cdot (b-d)}{2}} + c \tag{5.3.7}$$

Substituting a value of Eq. 5.3.7 into Eq.5.3.5, then Failure load P can be earned. For plastic region, the m can be represented as the unit plastic moment m_p, the plastic moment resistance can be written as Eq.5.3.9.

$$m_p = \frac{h^2 \cdot \sigma_y}{4} \tag{5.3.8}$$

$$P = \left(\frac{b}{a-c} + \frac{2a}{b-d} \right) \cdot h^2 \cdot \sigma_y \tag{5.3.9}$$

Thus, P in Eq.5.3.9 can be regarded as the design strength for the plate illustrated in Fig.5.3.1. However, in case of CFT Column, its plate in tension is able to develop tensile membrane action that increases the load capacity past its bending strength indicated in Eq.5.3.9 with the considerable support of the sidewalls. By using principles of virtual

work, it is possible to relate the failure load of the CFT's steel plate to tis defelction. Jones et al. (2007) use this approach to develop equations to predict the membrane action capacity of the CFT column's plate, and suggested following equations for the design strength for the CFT column's plate ($F_{Rd,plate}$).

$$F_{Mem,rows} = 2 \cdot f_y \cdot h \cdot \delta_m \cdot \left(\frac{d - 2 \cdot d_b}{\sqrt{b(b-d)/8}} + \frac{2}{3} - \frac{d_b^3}{12 \cdot L_{Diag}^3} \right) \times n \qquad (5.3.11)$$

$$F_{Mem,Group} = 2 \cdot f_y \cdot h \cdot \delta_m \cdot \left(\frac{d - 2 \cdot d_b}{\sqrt{b(b-d)/8}} + \frac{c - n \cdot d_b}{(b-d)/2} + \frac{2}{3} - \frac{d_b^3}{12 \cdot L_{Diag}^3} \right) \qquad (5.3.12)$$

$$F_{Rd,plate} = Min\left[F_{Mem,Rows}; F_{Mem,Group} \right] \qquad (5.3.13)$$

where f_y is material yield stress, h is column thickness, δ_m is cross section deflection due to membrane action and L_{Diag} is diagonal length along the membrane action mechanism.

Now, full force-deflection curve of CFT column's plate with end-plate effect can be earned with the tension stiffness (Eq.4.4.2) and design strength for the CFT column's plate (Eq.5.3.13). And these results had been compared to experimental data of table 4.3.1 at Figs.5.3.2, 5.3.3 and 5.3.4.

Fig. 5.3.2 Result(displacement) comparison with proposed equation and experimental data for case E13

Fig. 5.3.3 Result(displacement) comparison with proposed equation and experimental data for case E16

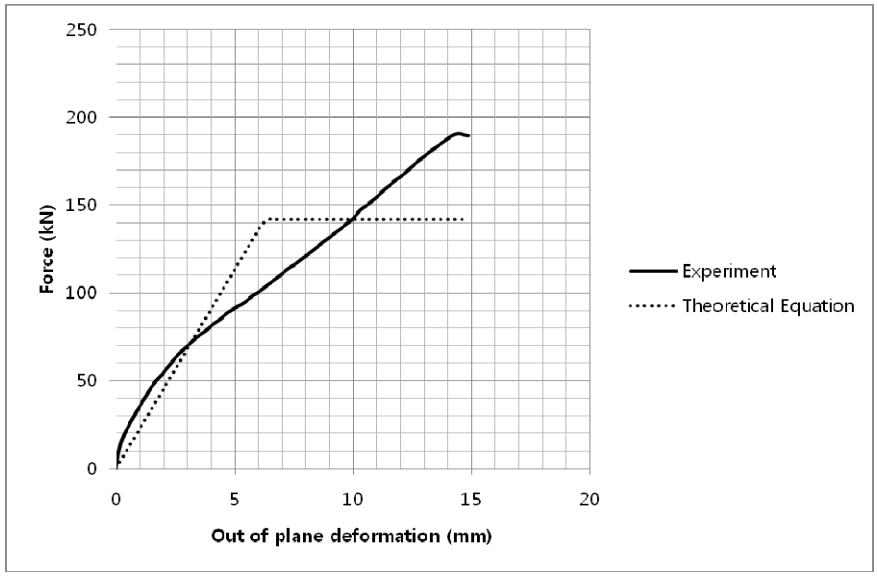

Fig. 5.3.4 Result(displacement) comparison with proposed equation and experimental data for case E19

5.3.2 The characteristics of the CFT column in shear

The characteristics of the CTF column in shear can be earned through using strut-and-tie method and STM model for this is illustrated at Fig.5.3.5. In case of longitudinal tension force and compression force in Fig.5.3.5, they are contributed to the column action due to the force through the beam. In case of transverse tension force in Fig5.3.5, it is induced by bolt force transferred by the CFT column wall as shown at Fig.5.3.6. And transverse compression force in Fig5.3.5 was induced by the beam directly. These above four forces are contributing to create the strut in column as indicated at Fig.5.3.5.

By the lower bound solution using arch action, the STM model of Fig.5.3.5 can be represented as Fig.5.3.7 for steel and Fig5.3.8 for steel tubular section and concrete

section, where r is height of loaded area, j is the length to satisfy the right angle of strut, z is the moment arm and b is the width of CFT column.

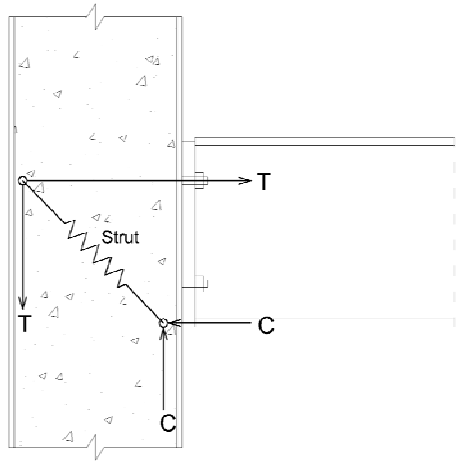

Fig. 5.3.5 STM model for CFT column in shear

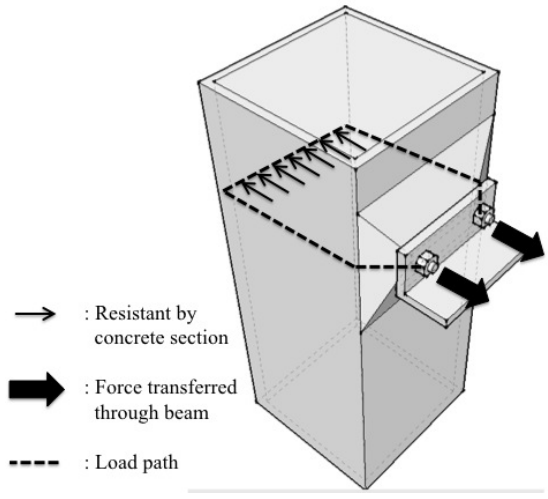

Fig. 5.3.6 Load path for transverse tension force by bolts

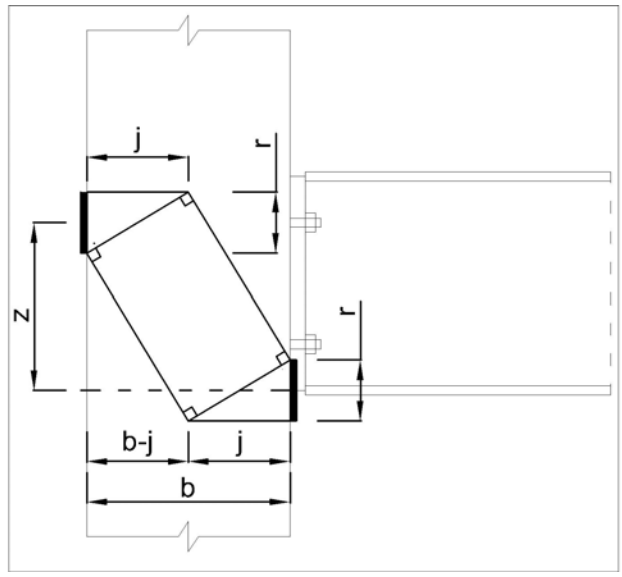

Fig. 5.3.7 STM model dimension for steel section of CFT

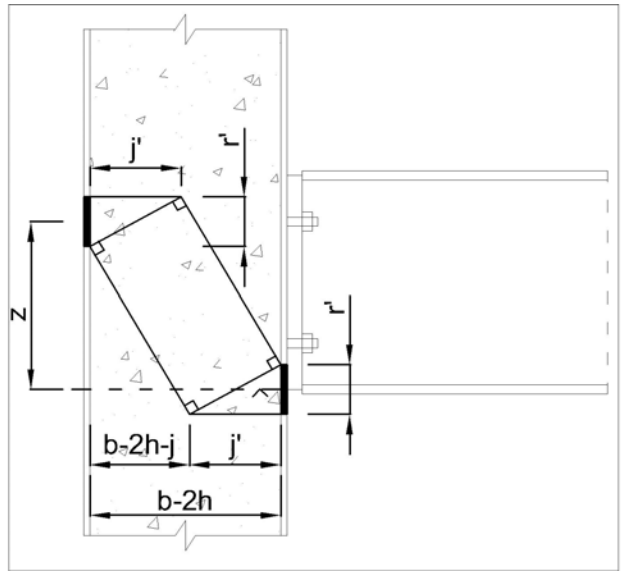

Fig. 5.3.8 STM model dimension for concrete section of CFT

To define the stiffness and strength of each section, the value of j and r need to be defined first. In case of j, it can be defined as b/2 for steel section and (b-2h)/2 for concrete section because the maximum load is obtained at these values. For the value r, it can be earned through the geometry of Fig5.3.9. The relationship between j and r can be found in the condition that sum of angle A and B should be π/2.

$$a\tan\left(\frac{z}{b-j}\right)+a\tan\left(\frac{r}{j}\right)=\frac{\pi}{2} \tag{5.3.14}$$

With this relationship value r and r' can be represented as follow:

$$r=j\times\tan\left(\frac{\pi}{2}-a\tan\left(\frac{z}{b-j}\right)\right) \tag{5.3.14}$$

$$r'=j'\times\tan\left(\frac{\pi}{2}-a\tan\left(\frac{z}{b-2h-j'}\right)\right) \tag{5.3.15}$$

With above values for j and r, the shear strength for steel tube and concrete section can be defined as follow, respectively:

$$F_{Rd,s,steel}=r\cdot b\cdot f_s \tag{5.3.16}$$

$$F_{Rd,s,conc}=r'\cdot(b-2h)\cdot f_c' \tag{5.3.17}$$

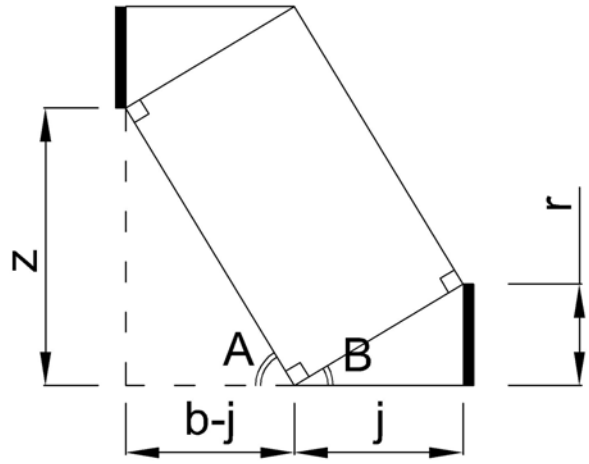

Fig. 5.3.9 The geometry of STM model for CFT column in shear

The shear stiffness of each section can be determined by the compression stiffness of the strut. And it can be easily calculated with the formula EA/L and geometry of Fig.5.3.7 and Fig.5.3.8:

$$k_{s,steel} = E_s \cdot \left(\sqrt{j^2 + r^2} \cdot 2h \right) / \sqrt{(b-j)^2 + z^2} \tag{5.3.18}$$

$$k_{s,conc} = E_c \cdot \left(\sqrt{j'^2 + r'^2} \times (b-2h) \right) / \sqrt{(b-2h-j')^2 + z^2} \tag{5.3.19}$$

To apply these strength and stiffness equation to CFT column, these characteristics need to be combined with using the parallel configuration of component method. With this principle in chapter 2.1, the shear strength and stiffness of the CFT column can be represented as follow:

$$F_{Rd,s} = F_{Rd,s,steel} + F_{Rd,s,conc} \tag{5.3.20}$$

$$k_s = k_{s,steel} + k_{s,conc} \tag{5.3.21}$$

5.4 The component assembly

The characteristics of each component of Fig5.1.2, the stiffness and the strength, can be obtained from the Euro code and the equations from this paper. And these values had been calculated at table 5.4.1. In this chapter, moment resistance and initial stiffness would be earned except the effect of (2) CFT column in compression which had not been investigated fully. Therefore, this component characteristics was set to infinite to demise the influence from those.

Using component method, the design resistance for tension($F_{Rd,t}$), compression($F_{Rd,c}$) and shear($F_{Rd,s}$) are the minimum value each section, respectively. In this example, $F_{Rd,s}$ should be the F_{R1}, $F_{Rd,c}$ is the minimum value of component (2) and (3), and $F_{Rd,t}$ is the minimum value of component (4), (5), (6) and (7). And the global design resistance(F_{Rd}) should be the minimum value of the these values as Eq.5.4.1.

$$\begin{aligned} F_{Rd} &= min\left[F_{t,Rd} + F_{slab,Rd}\,;F_{c,Rd}\,;F_{s,Rd} \right] \\ &= min\left[154.7+116.4;287.246;226.2\right] = 226.2kN \end{aligned} \tag{5.4.1}$$

Table 5.4.1 Design strength and Stiffness coefficients for components

	Components	Design Strength(kN)	Stiffness Coefficient(mm)
(1)	CFT column in shear (conc)	$F_{Rd,1}$ =226.2	$k_{1,c}$=51
	CFT column in shear (steel)		$k_{1,c}$=9
(2)	CFT column in compression	$F_{Rd,2}$= ∞	k_2=∞
(3)	Beam flange in compression	$F_{Rd,3}$=287.246	k_3=∞
(4)	End plate in bending	$F_{Rd,4}$=154.765	k_4=13.877
(5)	Bolt row in tension	$F_{Rd,5}$=180.8	k_5=6.525
(6)	Beam web in tension	$F_{Rd,6}$=232.8	k_6=∞
(7)	Column plate in tension	$F_{Rd,7}$=202.6	k_7=4.15
(8)	Slab reinforcement in tension	$F_{Rd,8}$=116.4	k_8=0.426

Lever arm for resistance calculation can be earned through correlation between design resistance of tension, compression and slab as indicated at Eqs.5.4.2 and 5.4.3.

$$F_{Rdo} = min\left[F_{t,Rd} + F_{slab,Rd}; F_{c,Rd}\right] = min\left[154.7 + 116.4; 287.246\right] = 271.1kN \quad (5.4.2)$$

$$F_o = \frac{F_{Rdo}}{F_{slab,Rd}} - 1 = \frac{271.1}{116.4} - 1 = 1.329 \quad (5.4.3)$$

$$z = \frac{1 + F_o \cdot \left(z_2 / z_1\right)^2}{1 + F_o \cdot \left(z_2 / z_1\right)} z_1 = \frac{1 + 1.329 \times 0.5416^2}{1 + 1.329 \times 0.5416} \times 305.4 = 244.32mm \tag{5.4.4}$$

Therefore, Plastic moment resistance should be as follow:

$$M_{Rd} = F_{Rd} \cdot z = 226.2kN \times 244.32mm = 55.2kN \cdot m \tag{5.4.5}$$

And elastic resistance can be obtained by the product of the plastic moment resistance and two third parts.

$$M_{e,Rd} = \frac{2}{3} \cdot M_{Rd} = 36.8kN \cdot m \tag{5.4.6}$$

The stiffness of each section can be obtained by Eq.2.1.2 because all the springs are connected as parallel. In this example, shear stiffness and compression stiffness can be earned easily through simple comparison, and tension stiffness except slab component would be earned as follow:

$$k_t = \frac{1}{\frac{1}{k_4} + \frac{1}{k_5} + \frac{1}{k_6} + \frac{1}{k_7}} = \frac{1}{\frac{1}{13.877} + \frac{1}{6.525} + \frac{1}{\infty} + \frac{1}{4.15}} = 2.14mm \tag{5.4.7}$$

Because the location of bolt and the reinforcement of slab is different, the lever arm

of tension zone should be integrated to single value with using Eq.2.1.9.

$$z_{eq} = \frac{k_8 z_1^{\,2} + k_t z_2^{\,2}}{k_8 z_1 + k_t z_2} = \frac{0.426 \times 305.4^2 + 2.14 \times 165.4^2}{0.426 \times 305.4 + 2.14 \times 165.4} = 203mm \qquad (5.4.8)$$

Substituting the value of 5.4.8 into Eq.2.1.8, the stiffness for tension zone can be obtained as follow:

$$k_{eq} = \frac{k_8 z_1 + k_t z_2}{z_{eq}} = \frac{0.426 \times 305.4 + 2.14 \times 165.4}{203} = 2.38mm \qquad (5.4.9)$$

Finally, the global stiffness of this semi-rigid joint can be obtained with substituting values of Eq.5.4.8 and Eq.5.4.9 into Eq.2.1.3.

$$\begin{aligned} S_{j,ini} &= \frac{z^2}{\sum \frac{1}{E_i \cdot k_i}} = \frac{z_{eq}^2}{\frac{1}{E_c \cdot k_{eq}} + \frac{1}{E_c \cdot k_c} + \frac{1}{E \cdot k_s}} \\ &= \frac{203^2}{\frac{1}{210 \cdot 10^3 \cdot 2.38} + \frac{1}{\infty} + \frac{1}{29 \cdot 10^3 \cdot 51 + 210 \cdot 10^3 \cdot 9}} = 17935kN \cdot m \end{aligned} \qquad (2.1.3)$$

Chapter 6. Conclusions

This paper is aiming to obtain the tension stiffness of the CFT column's plate to apply the component method to the CFT column for more efficient design and precise analysis.

The proposed equation is theoretically based on the plate theory with the assumption of the contributed column area and loaded area by bolt. And numerical analysis using Abaqus computer program had been conducted to figure out those assumptions. As a result, the length a which is assumed for analyzing steel tube as a plate have simple conditions for its longitudinal direction was determined as 1.0*b. In addition to this, the bolt arrangement modification factor Ψ was also determined by numerical analysis to narrow the gap between the assumption and the actual case. The numerical analysis had been conducted for 5 cases same as the former, and it defined modification factor Ψ as 1.25 for single bolt row, 1.66 for double bolt rows. And next, adjusted theoretical equation and numerical analysis model had been developed to consider the end-plate effect to the existing model. The result of these equations and numerical models had been verified by the comparison with experimental data. With these procedures, the equation for the tension stiffness of the CFT column's plate suggested as follow:

$$k_{p,CFT,e} = \psi \cdot \kappa \cdot \frac{D}{b^2} \tag{4.4.2}$$

where Ψ is the modification factor, κ is the coefficients for bolt arrangement as table

4.4.1, ν is the poisson's ratio, E is the young's modulus h is the thickness of the steel tube and b is the width of the steel tube.

This suggested equation is far simpler than Eq.2.3.4 suggested by Neves and Gomes (1996) with precise results. Therefore, applying to this equation to the component method is expected to design and analyze the beam-CFT column joint(semi-rigid joint) more efficiently and precisely.

References

Abaqus Analysis User's Manual Ver. 6.7

Abaqus Theory Manual Ver. 6.7

Ansel C. Urugal. "Stresses in Plate and Shells 2nd edition." WCB McGraw-Hill, 1999.

Ashley Y.Park "Semi-rigid joints to tubular column and their use in semi-continuous frame design", University of Manchester, England, 2012

British Steel. CIDECT Report No. 6F-13A/96 "Flowdrill Jointing System Part 1 Mechanical Integrity Tests" Corby, England, 1996

British Steel. CIDECT Report No. 6F-13B/96 "Flowdrill Jointing System Part 2 Mechanical Integrity Tests" Corby, England, 1996

Eurocode 3: Design of steel structures - Part 1-8: Design of joints, CEN, 2003

Gerald Huber "Non-linear calculations of composite sections and Semi-continuous joints", Ernst & Sohn

Gerald Huber "Semi-continuous beam-to-column joints at the millennium tower in Vienna, Austria.", University of Innsbruck, Innsbruck, Austria

Jones, M., & Wang, Y., "Tying behavior of fin-plate connection to concrete-filled steel tubular column - Development of a simplified calculation method", Journal of Constructional Steel Research, pp.1-10, England

Liu, Y. et al., "Response and component characterization of semi-rigid connections to tubular column under axial loads", Imperial college, London, UK, 2012

de Lima L.R.O et al "Experimental and mechanical model for predecting the behavior of minor axis beam-to-column semi-rigid joints", Pontifical Catholic University of Rio de Janeiro, Rio de Janeiro, Brazil, 2002

Nielsen, "Limit Analysis and Concrete Platicity", CRC press, 1999

Neves L.C. and Silva L.A.P et al, "Experimental behavior of end plate I-beam to concrete- filled rectangular hollow section column joints", University of Coimbra, Portugal, 2003

Silva L.A.P et al "Evaluation of ductility in steel and composite beam-to-column joints: Analytical evaluation", University of Coimbra, Portugal, 2003

Silva L.A.P, Neves L.F.N and Gomes F.C.T "Rotational Stiffness of Rectangular Hollow Sections Composite Joints", University of Coimbra, Portugal, 2003

Rudolph Szilard. "Theories and Applications of Plate Analysis." John Wiley & Sons, INC., 2004.

Zeotemeijer P. "Summary of the research on bolted beam-to-column connections". TU-Delft report 26-6-90-2, TU-Delft, Delft, Netherland, 1990

국문 초록

Component method 적용을 위한 CFT 기둥 강재판의 인장 거동 특성

김상우
건축학과 건축구조전공
서울대학교 대학원

이 연구에서는 CFT 기둥을 이용한 보-기둥 접합부를 보다 정확하고 효율적으로 설계 및 해석하기 위하여 Component method를 이 접합부에 적용하고자 하였으며, 이를 위해 CFT 기둥 강판의 인장 강도를 구하고자 한다.

길이 방향의 길이가 가로방향 길이에 비해 매우 큰 CFT 기둥 강판의 인장 강도를 plate theory를 통해 구하기 위하여 실제 강판과 처짐에 있어 비슷한 거동을 하며 한정된 길이방향의 길이를 가지는 강판을 구성하였다.

이 강판은 세로방향으로는 강접합, 가로방향으로는 단순접합의 경계조건을 가지며, 가로길이는 기둥의 폭, 세로길이는 미지수 a로 설정하였다. 실제 기둥의 거동과 동일한 거동을 같게 하는 미지수 a를 구하기 위하여 가정된 강판에 대한 이론식을 plate theory를 통하여 도출하고, 이를 수치해석결과와 비교하였다. 그 결과, a를 기둥의 폭에 비례하는 값으로 나타낼 수 있었으며, 수치해석 결과를 통해 볼트의 열 개수에 따른 수정계수를 도출하였다. 이에 더불어, 강판의 변형에 영향을 주는 end-plate 효과를 고려하기 위하여 제안된 이론식과 유한요소해석 모델을 변형하여 최종적으로 CFT 기둥의 인장강도에 대한 이론식이 도출되었으며, 이 이론식을 실험 결과 및 유한요소해석 결과와 비교하여 타당성을 검토하였다.

하중의 영향을 받는 강판의 길이(가정된 강판의 세로길이)는 강판 폭의 0.7배로 결정되었으며, 가정된 하중이 가해지는 넓이에 대한 오차를 줄이기 위하여 수정계수를 이론 식에 도입하여 최종 강도식을 제안하였다.

또한 제안된 강도식을 반강접 보- CFT 기둥 볼트 접합부에 도입하여 component method를 이용한 설계의 예를 제시하였다.

Keywords: Component method, CFT column, Plate theory, tension stiffness, Experiment, Numerical Analysis, Semi-rigid connection

학번: 2011-23296

감사의 글

어느덧 석사생활을 마무리 짓고, 이렇게 논문을 완성하여 감사의 글을 쓰고자 하니 그간 지내왔던 2년의 시간들이 주마등같이 지나가는 것 같습니다. 석사생활을 하면서 정말 많은 지식을 배웠고 저 자신을 보다 발전시킬 수 있었지만 한편으로는 제 지식의 부족함과 학문적 도전의식을 느끼기도 하였습니다. 훌륭하신 교수님들로부터 들은 수업을 통해 얻은 것도 너무나도 많았지만, 대학원에서 얻은 가장 큰 수확은 제 자신의 공부를 하고 저 자신의 논리를 가질 수 있는 시발점을 갖게 된 점인 것 같습니다. 대학원에서 다양한 영역을 공부하고 그것에 대해 혼자 논문을 찾아 이해하고 이에 제 생각을 더해 보고자 하였는데, 이러한 과정을 통해 학문이란 것이 무엇인지에 대하여 미숙하게나마 알게 된 것 같습니다. 그리하여 저에게 이러한 소중한 경험을 갖게 해주신 분들께 감사의 말씀을 드리고자 합니다.

먼저 항상 못난 저를 위해 든든한 버팀목이 되어주시는 부모님께 감사를 드립니다. 부모님이 계시기에 지금의 제가 있는 것이기에 항상 감사함을 잊지 않고 보다 더 열심히 노력하고 있습니다. 보다 자랑스러운 아들이 되어 부모님의 보람이 되고, 부모님께 항상 새로운 즐거움을 드리고 싶습니다. 그리고 항상 저를 먼저 생각해주고 아껴주는 누나, 항상 모범적이신 매형, 언제나 절 아껴주셨던 할머님, 항상 감사합니다.

저에게 교수님이라는 권위보다는 스승으로써 가르쳐주신 홍성걸 교수님께 진심으로 감사를 드립니다. 덕분에 교수님으로부터 정말 많은 것을 배웠고, 교육 그 이상의 것도 느낄 수 있었습니다. 그리고 항상 좋은 수업으로 이끌어 주신 박홍근 교수님, 학자로서의 풍채를 지니신 이철호 교수님, 인자하시고 열정적이신 강현구 교수님께 모두 감사를 드립니다.

제 연구실 생활의 전부인 것 같은 임우영 박사님, 학문적으로는 열정적이지만 따뜻한 감성을 가진 어진 누나, 연구실의 대들보이자 빛과 소금 같은 존재인 지형 누나, 지금도 속을 알 수 없지만 항상 친절하게 대해준 민수형, 항상 밝고 쾌할하신 양희 누나, 꼼꼼하고 항상 열심히 이신 성훈이형, 졸업하셨지만 올곧고 자유분방한 태욱이형, 항상 주변을 즐겁게 하는 혜진이, 센스 있는 은재, 연구실 차세대 에이스 유선이, 착하고 매사에 열심히인 지현이, 4차원 매력을 지닌 도영이 그리고 구조재료 실험실 선, 후배 모든 분들 감사합니다.

논문을 쓰면서 여러 방면으로 도와준 은근히 천재 성용이형, 대학 동기이지만 대학원에서 더 편해진 대경이, 항상 웃음으로 대해주신 상희 형, 유일한 동기이고 언제나 듬직한 철구, 못난 형이라도 잘 따라준 장운이, 현준이, 승표, 호준이 그리고 다른 연구실 모든 분들께도 감사의 말씀을 전합니다.

'

2년이라는 짧지 않은 시간 동안 많은 것을 얻게 도와주신 모든 분들께 감사를 표하며, 항상 겸손한 마음가짐을 가지고 학문에 정진하여 그 도움에 보답하도록 하겠습니다.